EXTENDED KALMAN FILTER (EKF)-BASED MODULAR-STACK VANADIUM REDOX FLOW BATTERY (V-RFB) PREDICTION MODEL DEVELOPMENT FOR REDUCING ELECTRODE CONTACT RESISTANCE AND PARALLELIZATION CURRENT

MOHD RUSLLIM MOHAMED

RDU150123 / FRGS
FUNDAMENTAL RESEARCH GRANT SCHEME (FRGS) FINAL REPORT

UNIVERSITI MALAYSIA PAHANG

UNIVERSITI MALAYSIA PAHANG

DECLARATION OF THESIS AND COPYRIGHT

Author's Full Name :
Date of Birth :
Title :
Academic Session :

I declare that this thesis is classified as:

☐ CONFIDENTIAL	(Contains confidential information under the Official Secret Act 1997)*
☐ RESTRICTED	(Contains restricted information as specified by the organization where research was done)*
☒ OPEN ACCESS	I agree that my thesis to be published as online open access (Full Text)

I acknowledge that Universiti Malaysia Pahang reserves the following rights:

1. The Thesis is the Property of Universiti Malaysia Pahang
2. The Library of Universiti Malaysia Pahang has the right to make copies of the thesis for the purpose of research only.
3. The Library has the right to make copies of the thesis for academic exchange.

Certified by:

@DR.MRM

____
('s Signature)

771026-03-6323

____
New IC/Passport Number
Date:

NOTE : * If the thesis is CONFIDENTIAL or RESTRICTED, please attach a thesis declaration letter.

DECLARATION

I hereby declare that the work in this thesis is based on my original work except for quotations and citations which have been duly acknowledged. I also declare that it has not been previously or concurrently submitted for any other degree at Universiti Malaysia Pahang or any other institutions.

@DR.MRM

____

(Signature)

Full Name : Mohd Rusllim Mohamed

ID Number : 0102

Date : 10 August 2019

ACKNOWLEDGEMENTS

We would like acknowledge Ministry of Education Malaysia and Universiti Malaysia Pahang for giving the fund of Fundamental Research Grant Scheme.

We also would like to thank all our MSc. Students benefited from this grant and has completed their studies i.e. Suhailah Sujali dan Siti Fadhilah Mohamed Ibrahim which their content of the thesis has been transferred in this final report.

ABSTRAK

Bateri Vanadium Redox (V-RFB) adalah sejenis bateri aliran boleh dicas semula yang menggunakan ion vanadium dalam keadaan pengoksidaan yang berlainan. Ia mengalami tindak balas pengoksidaan dan pengurangan semasa proses pelepasan dan caj di anod dan katod. Pada masa ini, terdapat kekurangan kajian penerbitan mengenai model litar elektrik untuk V-RFB. Model elektrokimia biasanya digunakan untuk mewakili bateri disebabkan oleh perinciannya dalam proses elektrokimia, bagaimanapun, model ini tidak sesuai untuk mengenal pasti kelakuan elektrik V-RFB. Anggaran parameter pada model bateri adalah proses untuk menyesuaikan litar bersamaan ke dalam bateri. Tesis ini membentangkan litar elektrik bersamaan yang terdiri daripada litar sebenar dan anggaran untuk V-RFB serta tingkah laku hidrodinamik bateri aliran Vanadium redox (V-RFB) dengan menggunakan model dinamik cecair pengkomputeran 3D (CFD). Tujuan projek ini adalah untuk mencadangkan litar elektrik bersamaan untuk V-RFB yang mewakili ketulenan yang baik untuk analisis dan reka bentuk litar dan untuk mengkaji kuasa pam (penggunaan tenaga pam) dan pengagihan aliran elektrolit yang diperlukan dalam sel. Untuk litar bersamaan, litar sebenar terdiri daripada potensi sel litar terbuka, dua cawangan Resistor-Capacitor (RC), siri RC, rintangan dalaman, dan induktor. Dari litar, beberapa parameter disusun untuk membina litar anggaran terdiri daripada potensi sel litar terbuka, impedans cawangan RC dan rintangan dalaman dengan induktor. Litar anggaran dibina untuk menunjukkan hasil yang kurang kompleks dan menjimatkan masa. Penambahan Kalman Filter (EKF) digunakan untuk penganggaran parameter untuk kedua-dua litar. Litar sebenar dan anggaran diambil dengan sewajarnya. Hasil simulasi melalui algoritma rekursif EKF setiap parameter dari kedua-dua litar menunjukkan mendekati mantap dengan kesalahan 0.6% dan 2.0%. Jadi, ia terbukti bahawa kedua-dua litar ini boleh disesuaikan untuk V-RFB. Di sisi lain, tiga geometri sel berbeza dari sel V-RFB, iaitu reka bentuk sel persegi, rombus dan pekeliling dinilai pada tiga kes berbeza iaitu tiada saluran (kosong) saluran, saluran selari dan saluran serpentin. Selain itu, kerja telah diperluaskan dalam pemasangan modular 100 cm^2 V-RFB. Pemasangan modular telah dibangunkan dan diuji untuk memerhatikan kuasa pam dalam timbunan dalam tiga reka bentuk yang secara langsung berkaitan dengan prestasi sel berkenaan dengan pengagihan kuasa dan kehilangan kuasa. Berdasarkan penemuan ini, sel mempamerkan ciri-ciri yang berbeza di bawah geometri berbeza sel V-RFB tanpa permohonan saluran aliran. Sebaliknya, berdasarkan skala geometri sel, hubungan antara kuasa pam dan geometri sel untuk 100 cm^2 V-RFB telah dibangunkan. Pengagihan aliran optimum dalam sel tanpa saluran aliran bendalir telah direkodkan; penggunaan pam tertinggi dan terendah masing-masing pada 25.6% dan 18.4%. Pengurangan kerugian kuasa sebanyak 53% telah dicatatkan sebagai saluran aliran selari telah digunakan untuk V-RFB. Korelasi yang berpadanan telah diperhatikan untuk V-RFB modular sebagai hasil daripada penambahan sel dan berpotensi untuk analisa lanjutan selanjutnya ke sel n. Kerja-kerja selanjutnya dikemukakan untuk kajian masa depan dalam kajian geometri V-RFB

ABSTRACT

Vanadium Redox Flow Battery (V-RFB) is a type of rechargeable flow battery that employs vanadium ions in different oxidation states. It undergoes oxidation and reduction reaction during discharge and charge process at anode and cathode. Presently, there are lack of publication studies on electrical circuit model for V-RFB. Electrochemical model is commonly use to represent battery due to its detailing in electrochemical process, however, the model is not suitable to identify electrical behavior of V-RFB. Parameter estimation on battery model is a process to fit an equivalent circuit into the battery. This thesis presents equivalent electrical circuit consists of actual and approximate circuit for V-RFB as well as hydrodynamics behavior of the Vanadium redox flow battery (V-RFB) by using 3D computational fluid dynamics (CFD) models. The aim of this project is to propose equivalent electrical circuit for V-RFB that represents excellent adaptableness to any circuitry analysis and design and to study the pump power (pump energy consumption) and electrolyte flow distribution required within the cell. For equivalent circuit, the actual circuit consists of an open-circuit cell potential, two Resistor-Capacitor (RC) branch, a series RC, internal resistance, and inductor. From the circuit, some of the parameters are lumped to construct approximate circuit consists of open-circuit cell potential, impedance of RC branches and internal resistance with inductor. Approximate circuit is built in order to present less complex result and save time. Extended Kalman Filter (EKF) is used for parameter estimation for both circuit. Actual and approximate circuit are derived accordingly. The simulation result through recursive EKF algorithm of each parameters of both circuits shows approaching steady with 0.6% and 2.0% errors, respectively. So, it proven that both circuit are adaptable for V-RFB. On the other hands, three different cell geometries of V-RFB cell, namely square-, rhombus- and circular cell designs are evaluated at three different cases i.e. no flow (plain) channel, parallel channel and serpentine channel. Furthermore, the work has been extended in modular stack of 100 cm^2 of V-RFB. The stack has been developed and tested to observe the pump power within the stack in the three designs which directly related to performance of the cell with respect to power distribution and power losses. Based on the findings, the cell exhibits different characteristics under different geometries of V-RFB cell at no flow channel application. Conversely, based on the scaling up of the cell geometry, the relationship between pump power and cell geometry for 100 cm^2 of V-RFB has been developed. Optimum flow distribution within the cells without fluid flow channels were recorded; highest and lowest pump consumption at 25.6% and 18.4% respectively. Extended reduction of power losses by 53% were recorded as parallel flow channels has been applied to the V-RFB. Proportionate correlations were observed for modular V-RFB as a result of scaling up of the cell and potential for further analysis of extension to the n^{th} cell. Further works are presented for future research in geometry study of V-RFB.

TABLE OF CONTENT

LIST OF TABLES

LIST OF FIGURES

CHAPTER 1

INTRODUCTION

1.1 Chapter overview

This chapter presents the following components: introduction of the project, problem statement, objective, contribution, scope of the project, and the thesis outline. Introduction will focus on energy storage, battery, V-RFB, and Kalman filter. Objectives are discussed in the project's aim, while the flow of the project from where it began to the end is explained in the project's scope. Finally, the thesis outline which briefly describes each chapter of the thesis concludes the chapter.

1.2 Introduction

Energy is one of the most important properties in human lives. While it presents everywhere and it has the capability to make changes to the surrounding, it can neither be created nor destroyed as stated in the law of conversion of energy and statement for the First Law of Thermodynamic (Law & Law, 2009). The production of energy that is captured for a later use is known as energy storage. There are many types of energy storage and electrochemical energy storage is one of it (Oberhofer, 2012). Electrochemical energy storage is a conversion of chemical to electricity potential and vice versa for storage. This storage describes various types of batteries and almost all of them are technically advanced for application (Iec, 2009).

Batteries store energy from hours to days, the storage capacity can be extended without the need to upgrade the power generation system so it is easily scalable. There are two basic types of batteries; primary (non-rechargeable) and secondary (rechargeable) batteries (Vutetakis, 2001). Secondary or rechargeable battery is the type of electrical battery which is charged by applying electric current and is discharged when being used (Doughty, Butler, Akhil, Clark, & Boyes, 2010).

Studies have found that energy storage is significant and is a potential solution to stabilise load level and strengthen the power network. There are various types of energy storage that transfer and distribute energy, such as compressed air energy storage (CAES), flywheel energy storage (FES), pumped hydro energy storage (PHES), superconducting magnetic energy storage (SMES), and battery energy storage (BES) (Mahlia, Saktisahdan, Jannifar, Hasan, & Matseelar, 2014). There are many possible techniques or types of storage in this world, but this work focuses on one of the battery energy storage technologies. Among various battery energy storage technologies, vanadium redox flow battery (V-RFB) offers promising advantages because of its supreme features including effective and simple operation, capability of high power independent of energy and power capacities, fast response and recharging contenders, excellent chemical stability that shows an extremely long-round-trip cycle, operationality at room temperature, long discharge times exhibited for highly reversible redox kinetics, suitable for large-scale applications, and reasonable and controlled maintenance cost compared to conventional battery (Miyake & Tokuda, 2001; Park, Jeon, Ryu, & Hwang, 2017).

Vanadium Redox Flow Battery (V-RFB) is a rechargeable flow battery that employs vanadium ions to store chemical potential energy in different oxidation states. It undergoes oxidation and reduction reaction during discharge and charge processes at anode and cathode. Both sides of V-RFB system selective membrane use vanadium compound because it is fundamentally reliable and it has simple maintenance procedures which are different from the other flow batteries (Blanc & Rufer, 2010). By eliminating cross-contamination the electrolyte does not require to be changed, it lasts indefinitely and it is highly efficient as the charge acceptance of the system is optimal and nominal (Tokuda et al., 1998). Hence, it lasts long and there are no losses of system integrity. More attention has been given on V-RFB rather than other chemical batteries because V-RFB has unique features which consist of decoupled energy storage and power component. These features give V RFB an independent control of capacity and power and are attractive for optimisation of power and energy in Electric Vehicle (EV) applications (Rusllim Mohammad, Sharkh, & Walsh, 2010). In addition, V-RFB employs the same element in both the positive and negative half-cells, so it does not affect battery capacity as the problem of cross-contamination of ions is avoided.

Battery's circuit need to be model properly. It is vital to acquire precise simulation and result. By modelling complex circuit into simplify form, analyzation can take place smoothly. Furthermore, it will reduce cost and time. A proper way to describe dynamic process of chemical reaction on the system electrodes of V-RFB is based on electrochemical model (Dees, Battaglia, & Bélanger, 2002; Shah & Walsh, 2009; Caiping Zhang, Liu, Sharkh, & Zhang, 2009). However, to describe V-RFB electrical behaviour is not well appropriate due to the requirement of battery chemical parameters. Thus, an equivalent electrical circuit that signifies excellent adaptability and simple realization of V-RFB system is required.

Figure 1.1 shows a concept diagram for the V-RFB configuration. The flow battery consists of two electrochemical half-cells (anode and cathode parts) separated by ion exchange membrane. A pump is used to circulate electrolyte through the cell stack. Most of the research and development are focused on the active material (P. Leung et al., 2016), design installation and cell configuration (Blanc, Member, & Rufer, 2008), improving poor kinetic reaction conductivity (A. C. Khor et al., 2016), redox couples(P. K. Leung, Mohamed, Shah, Xu, & Conde-duran, 2015), and battery characterisation (Mohamed, Leung, & Sulaiman, 2015a). Figure 1.2 depicts the time frame of flow battery development which was reviewed extensively by Skyllas-Kazakos and her team (Rychcik & Skyllas-Kazacos, 1988) up to 2000s and later continued by Rahman (Rahman & Skyllas-Kazacos, 2009) and more detail discussion on 3D V-RFB modelling and engineering aspect reviewed by Yin (Yin, Gao, Guo, & Tang, 2014) and Arenas (Arenas, León, & Walsh, 2017).

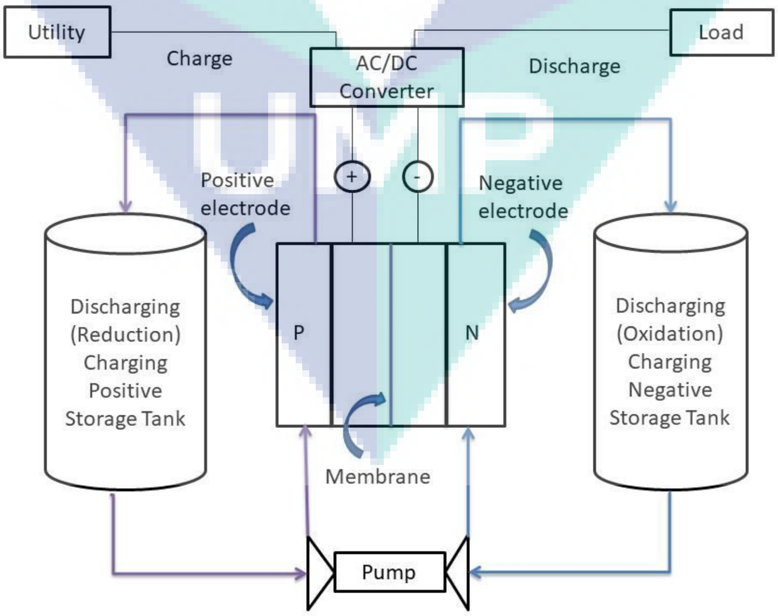

Figure 1.1 V-RFB configuration

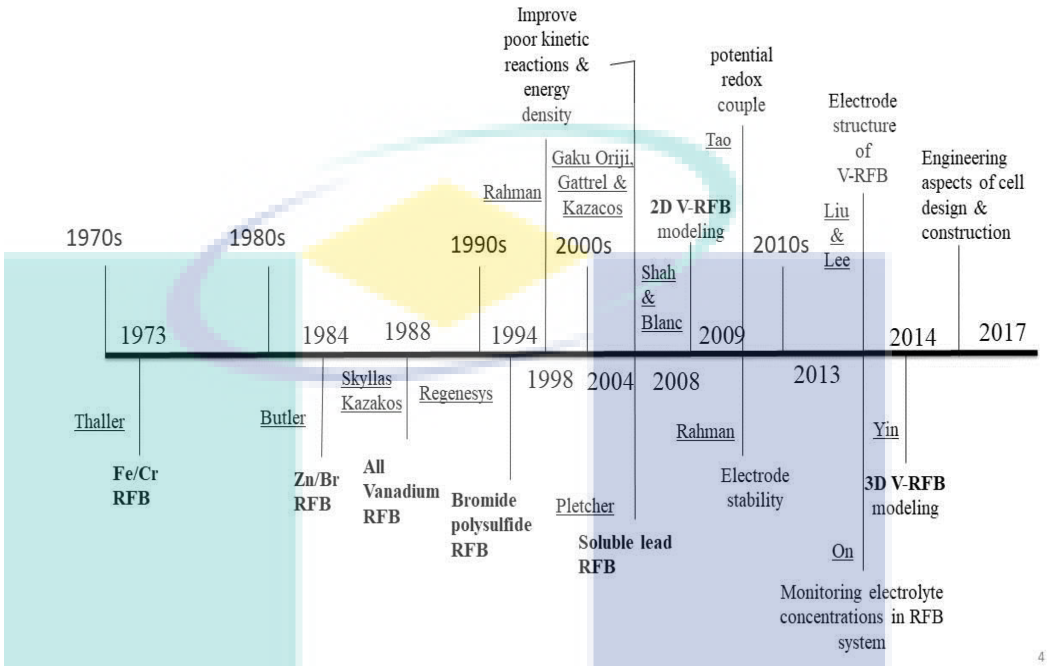

Figure 2.2 Time-line for development RFB (not limited to)

Parameters in circuit model can be estimated in various method and Kalman Filter (KF) is one of the techniques. KF uses measured input and output to estimate the states of a system. It is an optimal and best linear estimator (Kleeman, 1996). In practice, Kalman Filtering illustrates best outputs, it is convenient form for online real time processing due to optimality and structure and also do not invert the measurement equations (Kleeman, 1996). There are many types of Kalman Filter such as Unscented Kalman Filter (UKF), and Extended Kalman Filter (EKF) (Banani, 2007). EKF is the common application of KF in a nonlinear system and is also known as one of the best estimators, from noisy data amount to filtering out the noise. EKF can gauge parameter data accordingly which results in time and cost saving.

1.3 Problem statement

Battery model can be categorized into thermal, electrochemical and electrical (Hall & Fasih, 2006). Electrochemical models suitable for optimization of the physical design aspects of electrodes and electrolytes (Dees et al., 2002; Zhang, Jiang, Zhang, & Sharkh, 2012). Electrochemical model is mostly accurate to represent battery due to its detailing in electrochemical process, however, the model is not suitable to identify electrical behavior of V-RFB. On the other hand, the equivalent circuit model has widely been used and researched due to its simplicity and adaptability on any circuitry design systems. Complexity to perform performance analysis of a battery is in proportional to the level of complexity of the equivalent circuit model (YIlmaz & Yuksek, 2008). Approximate circuit has a simpler model derivation, less computational time, and a smooth graph shape. The equivalent electrical circuit model publication studies for V-RFB are limited. To date, Chahwan et al. (2007) and M. R. Mohamed et al. (2013) proposed the equivalent electrical circuit for V-RFB. The former presented an equivalent circuit with parasitic and pumped losses with no Resistor-Capacitor (RC) network but there was no explanation on how the losses being estimated whereas the latter presented an equivalent circuit with a pair of RC network for a better representation within battery but there was no explanation on transient behaviour and mass transport. Parasitic inductance will have a major effect on battery model if a high current discharge is applied (Salerno & Korsunsky, 1998). Inductor contributes the transient behaviour of small voltage overshoot or undershoot (Yu & Yuvarajan, 2005).

Mohamed et al. (Mohamed, Sharkh, Ahmad, Seman, & Walsh, 2012) highlighted that V-RFB has been attracted by many researches; some are under field testing and demonstration stage, but information on cell construction, characterization and overall systems under study, etc. are still limited. Furthermore, the most critical part in V-RFB system is the construction of the cell; hence, deserve the most attention in analysis and manufacturing. Even though much research has been carried on V-RFB system, it should be noted that all previous studies of the use cell geometries for V-RFB with the channel and several patents, especially focusing on different designs, have limited scientific publication.

Estimation of parameters is carrying out in order to fit the equivalent circuit into battery. There is various method in estimating parameter such as Artificial Neural Network (ANN), spline technique, current change method and etc. ANN can be used for pattern extraction or complex trend that are hard to be noted by computer technique or human being. It can transform complicated and imprecise data to meaning derivation, however, ANN in a way are non-conventional method and the input output dataset are hard to identify because sufficient data training and testing are required in dataset

(YIlmaz & Yuksek, 2008). Spline technique is piece wise polynomials of degree ‘n’ and it easy to handle because represent by simple polynomials. Overshooting can occur at intermediate point as the high degree of polynomial is used. Although it good for behaviour of the actual system the overshooting will affect the estimation with the production of error (Wold, 1974). Current change method is a simple technique that changes the output current in order to obtain the transient waveform of the terminal voltage. It not a problem for the current change method to perform for single, small, and even larger stack of battery, however, the load current changes causes the related voltage change (Chang, 2013).

1.4 Objectives

The main objectives of the project are:

- To develop equivalent electrical circuit model for V-RFB with consideration of parasitic inductance.
- To propose approximate circuit as an alternative for actual circuit to represent general characterization of V-RFB.
- To estimate the equivalent electrical circuits model parameters by using EKF.

1.5 Scope of project

In this project, the overall scope is discussed in Figure 1.3. The project is expected to propose an equivalent electrical circuit along with the approximate circuit and EKF is used for parameter estimation of the circuit. The experimental data result was taken from Mohamed et al. (M. R. Mohamed, Ahmad, Seman, Razali, & Najib, 2013).

Energy storage can be formed into chemical, electrochemical, and thermal energy storage. Among these energy storages, the project will focus on electrochemical energy storage, because it is more stable, the oldest, and established.

Electrochemical energy storage is the place where various types of batteries were formed and found, for example, lead acid, nickel cadmium, RFB, lithium ion, and fuel cell. Rechargeable battery, RFB is chosen in the current study.

There are many types of RFB; iron/chromium, soluble lead acid, vanadium, zinc bromine, and vanadium bromine. Vanadium type of RFB is used because of its high energy density, less cross-contamination, and will not damage due to overly discharged.

In theoretical section, the project will be based on literature review and fundamental theory. For the circuit modelling section, the circuit model has been categories into thermal, electrical, and electrochemical model. For this project, the electrical circuit model is used because of its less complex model. The circuit model is divided into two; equivalent and approximate circuit. Equivalent circuit has widely been researched because it is simple and reliable. Approximate circuit is formed from the equivalent circuit because a less complex result can be presented. As for the simulation section, the circuits are verified by using EKF for parameter estimation in MATLAB. EKF can linearized the circuit and measure data though it is full of noise.

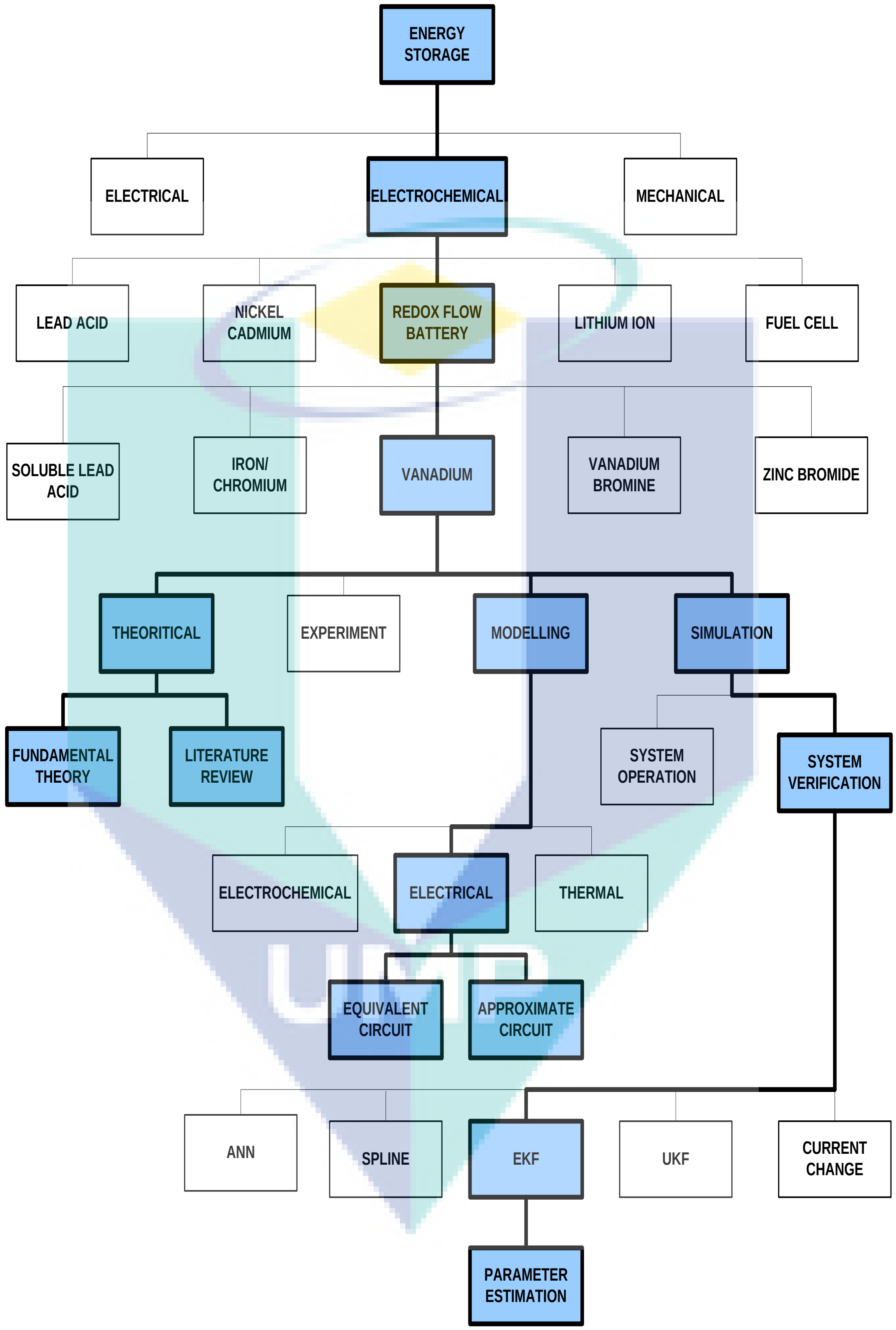

Figure 1.3 Fill of energy storage of equivalent circuit for V-RFB

CHAPTER 2

LITERATURE REVIEW

2.1 Chapter overview

This chapter discusses the literature review based on the project scope. Related articles published within the area were reviewed. Introduction, Energy storages are discussed and the focus is on the type of RFB. Description of RFBs leads to the explanation on the choice of V-RFB. From the chosen battery, the methods of parameter estimation were deliberated. The conclusion of the review of the literature leads to the need of the current project.

2.2 Introduction

The primary sources of energy like crude oil, natural gas, coal, nuclear, and hydroelectric are the main supplies for energy demand of all the population in the world. Fossil fuels are one of the energy sources that are used to generate electricity. However, the burning of fossil fuels leads to global warming due to the emission of CO_2 (Duncan, 1988), which has a damaging impact on the climate and the environment. Previous researches proved that the burning of fossil fuel has a major impact on global warming. Due of this, renewable energy sources have been introduced to meet the power demand and supply energy for future development; these sources have less environmental effects and reduce the dependency on fossil fuels (Denholm et al., 2010; Wei, Zhao, Zeng, Zhou, & Zeng, 2016).

The primary goal of renewable energy sources (RES) is to develop an alternative power supply. Generally, RES is from natural resources, such as wind and solar energy that have the potential to generate electricity for various industrial and domestic applications. However, RES is still unable to meet the electrical demands as the energy is meant for short-term storage and relies on the weather to work efficiently. Thus, there would always be on intermittent output because sources like the wind and the sun are unpredictable. To control the supply-demand imbalance, the energy storage system is needed to store the energy and give back the power at certain times during high power demands. Findings of energy storage technologies have provided insights for the development of large scale storage which is more efficient and has a longer lifespan (Haralambopoulos & Polatidis, 2003; Ipsakis et al., 2009; Painuly, 2001).

2.3 Energy storage

Mechanical Energy Storage

Mechanical energy storage stores energy by motion. Mechanical storage systems methods are hydraulic accumulator, compressed air energy storage (CAES) and flywheel energy storage. Hydraulic accumulator very important in generates electricity and had been installed worldwide but high cost and give a big impact to the environments and also lack of available sites (Hebner & Beno, 2002). CAES uses air as a storage due to viability and it has a large capacity, however it has efficiency with low round-trip and limitation of locations geographically (Iec, 2009; Koshizuka, Ishikawa, Nasu, Murakami, & Matsunaga, 2003; Oberhofer, 2012). Flywheel energy storage store energy through flywheel, it used to store grid energy as emergency power source(Hebner & Beno, 2002; Luo, Wang, Dooner, & Clarke, 2015; Mahlia, Saktisahdan, Jannifar, Hasan, & Matseelar, 2014).

Electrical Energy Storage

Electrical energy storage has two needs (Iec, 2009). First, as the electricity is generated at the same time it is expended and it will lead to unsatisfied demand if there is imbalance of supply and demand because the stability and the quality of the power supply will be damage. Second, location of electricity generation is from where it had been consumed. Electricity is vital for everyday routine because many tasks require the use of electricity. Magnetic energy storage; Superconducting Magnetic Energy Storage (SMES) and electrostatic energy storage; supercapacitor are basic categories in electrical energy storage (Blanc, 2016). SMES employs magnetic field energy. Although it is fast response, is able to discharge partially and fully, and also environmentally none hazard, the requirement in the cooling process reduces the efficiency, there are high expenses in manufacturing and maintenance, and it involves high energy losses (Koshizuka et al., 2003; Oberhofer, 2012). Supercapacitor stores energy in electrolytes solution between two solid conductors (H. Chen, Cong, et al., 2009). In comparison to conventional capacitor, high energy density can continuously charge and discharge, and can be used in many applications due to its long lifespan, and high efficiency; engine's starter, actuators, electric or hybrid-electric vehicles (H. Chen, Ngoc, Yang, Tan, & Li, 2009; Oberhofer, 2012)

Electrochemical Energy Storage

Electrochemical energy storage is the most established and oldest energy devices (H. Chen, Cong, et al., 2009). Various types of batteries are described from this energy storage and almost all of them are technologically mature for practical use (Iec, 2009). Battery is a conversion of chemical energy to electrical energy. In today's world, the use of battery is inevitable, from the households to the factories. Anode, cathode and electrolyte are three important components of a battery. There are two basic types of a battery; primary and secondary batteries (Vutetakis, 2001). Primary battery is not rechargeable, inexpensive, can be bought almost everywhere, easy to dispose, and poor performance at low temperature; for examples, alkaline battery, mercury battery, zinc-carbon, and etc. (Arnold, 2011; Singamsetti & Tosunoglu, 2012). Secondary battery is rechargeable, higher initial cost but lower operating cost, requires maintenance but a longer life cycle, durable, and better performance at low temperature; for examples, lead acid, lithium-ion, sodium-sulphur, redox batteries, and etc. (Antonucci & Antonucci, 2011; Singamsetti & Tosunoglu, 2012; Vutetakis, 2001).

2.4 Battery

Lead Acid Battery

Lead Acid(LA) battery is the type of energy storage battery that is commonly used commercially since 1859 and is applicable in both mobile and stationary applications (Iec, 2009). For over 150 years of development and experience, it has been considered as the most mature and oldest technology. It was widely used to substitute power supplies and is capable of delivering a high voltage of electricity at once but due to high lead density the life cycle and energy density is low (H. Chen, Ngoc, et al., 2009; Oberhofer, 2012;

Vutetakis, 2001). It has a large scale energy storage with low cost but it has limited life cycle and recharged ability, chemical reaction cause the corrosion to occur, people and animals can be affected by the exposure of lead this is because lead is toxic(H. Chen, Ngoc, et al., 2009; Oberhofer, 2012).

Nickel Cadmium

Nickel cadmium (NiCad) is considered as rechargeable alkaline battery with long life cycle. It can be developed in large scale application; telecommunication system. Compared to LA, it produces a higher energy with low maintenance cost and longer lifespan (H. Chen, Cong, et al., 2009; Pires, Romero-Cadaval, Vinnikov, Roasto, & Martins, 2014). In contrast, NiCad has a low cycle of life, and a high manufacturing cost (Alotto, Guarnieri, & Moro, 2014) and can be damaged by overcharging.

Lithium ions Battery

Lithium ion battery has a high energy density to store energy in a small space with a larger amount, high efficiency (range between 95% to 98% (Iec, 2009), and relatively long life span (H. Chen, Ngoc, et al., 2009). Lithium ions battery is an important storage in portable and mobile applications (Iec, 2009; Singamsetti & Tosunoglu, 2012). Further care should take place in order to recycle lithium because lithium can combust and some of the electrolytes are toxic (Díaz-González, Sumper, Gomis-Bellmunt, & Villafáfila-Robles, 2012; Pires, Romero-cadaval, Vinnikov, Roasto, & Martins, 2014; Singamsetti & Tosunoglu, 2012). It has a higher voltage per cell; 3.7V compared to lead acid; 2.0V, low energy lost, and a large amount of lithium and graphite are available. (Oberhofer, 2012; Singamsetti & Tosunoglu, 2012). On the other hand, lithium is expensive, the cell can be destroyed if fully discharged takes place, the cell will fail if not used, and lithium is combustible in contact with atmospheric moisture (Díaz-González et al., 2012; Oberhofer, 2012). In addition, the cost to construct it in a large scale is high due to circuit protection and packaging.

Fuel cell

Fuel cell (FC) is broadly used in various applications such as mobile and stationary (Pires, Romero-cadaval, et al., 2014). There are several types of fuel cell, which include polymer electrolyte membrane, alkaline, phosphoric acid, molten carbonate and solid oxide. FC is harmless to our body. In addition, it has low efficiency although it is conceptually the same with RFB (Alotto, Guarnieri, & Moro, 2013; Mohd R Mohamed et al., 2009). FC and batteries are different, FC consumes reactants which must be reloaded, whereas batteries store electrical energy chemically in a closed system. (H. Chen, Ngoc, et al., 2009; Pires, Romero-Cadaval, et al., 2014). Furthermore, when battery is charged or discharged the electrodes between the batteries are reactant change, while electrodes in FC are relatively stable (H. Chen, Cong, et al., 2009). FC is also difficult to handle and is costly.

Redox Flow Battery

Redox Flow Battery (RFB) is a device that stores electrochemical energy. The term redox is the combination of chemical reaction reduction and oxidation which undergo discharge and charge of electrochemical cell in which energy is stored in the electrolyte solution. One of the sources of direct current is RFB for various applications such as household and industry (Mahlia et al., 2014). There are many types of RFB such as zinc bromide, iron/chromium, bromide polysulphide, soluble lead acid, and V-RFB (Alotto et al., 2014; H. Chen, Cong, et al., 2009; Mohd R Mohamed et al., 2009). RFB has a longer life cycle and it is low in maintenance, for instance in circulating the electrolytes between the tanks and cell electrodes in RFBs only two low cost tanks are needed (Alotto et al., 2014; Oberhofer, 2012). However, RFB is unsuitable for mobile applications due to its low energy density, due to the electrolytes is conductive it disposed shunt current and extra losses can occur (Alotto et al., 2014).

Table 2.1 Comparison of energy storage technologies

Energy storage	Types	Efficiency	lifetime	Status	Problems
Mechanical	Hydraulic accumulator	85%	30 years	Commercial products	Exclusion area
	Flywheels	>90%	20 years	Prototypes in testing	Containment
Electrical	Super capacitors	95%	10 000 cycles	Some commercial products	Short period
	SMES	95%	30 years	Design concept	Short period
Electrochemical (battery)	LI-ion	>95%	1000 cycles	Commercial products	Thermal runaway
	V-RFB	85%	10 years	In test	Low energy density
	FC	40%	10-20 years	In test	Safety
	Lead acid	85%	2-10 years	Commercial products	Lead disposal

2.5 Overview of RFBs

In previous section, various energy storage technologies are presented. In electrical energy storage system, while it is able to operate at very high efficiency and has quick response for immediate backup power during interruptions but it has lower energy density and consumes high capital cost and it is actually suitable to use to complement other types of energy storage technologies. While, in mechanical energy storage safety is a major obstacle. Electrochemical energy storage technology is well suited for much large-scale application as it's provides flexible operation, high dynamics response, and high efficiency. Because of these unique features, electrochemical energy storage technology is really suitable emergency backup power and electric utility (Fujimoto et al., 2014).

Due to system power and capacity can be largely decoupled, RFB seem to be especially attractive system in electrochemical energy (Rusllim Mohammad et al., 2013). An RFB electrolyte is typically composed of three species: a solvent, supporting electrolyte, and the active species, or redox couple. Redox reactions are reduction and oxidation reactions in which the oxidation states of molecules change. RFB configuration; the characteristics and components are similar to those of fuel cell in the way that electrochemical energy is reserved in the tank that is occupied with active species.

Practically, the RFB mechanism consists of three segments including the cell stack, energy reserve tank, and flow circulation system. The cell stack consists of individual cells where every single cell contains a part where the electrochemical charge transfer reaction happens to store or release energy under redox reaction. Redox reaction is a reduction and oxidation process where the reduction involved the release of electron, and the oxidation involved the gain or recombination of the ions (Kear, Shah, & Walsh, 2012).

The reactants in the tank are recirculated through the redox flow cell. Pumps are used in flow batteries to help flow circulation by circulating the electrolyte for redox reaction which occurs through the cell stack and a porous electrode to generate electrons, which flow through the external circuit (Ponce de León et al., 2006).

On the negative side, flow batteries are rather complicated in comparison with other standard batteries as it is required much component which were pumps, sensors, control unit, reservoir tanks and electrolyte tube. The energy densities are relatively small compared to Lithium ion batteries.

2.6 Categories of RFB

RFB is one of the high potential batteries from electrochemical energy storage system that has been used in many applications because of its excellent characteristics such as good scalability, independent sizing of power and energy, and fast response. Multifarious types of redox flow battery like zinc–bromine (Zn-Br RFB), iron-chromium (Fe-Cr RFB), vanadium–vanadium (V-RFB) have great performance and outstanding role for stabilisation of both generation and grid load. They also offer a good system for electrical applications (Winsberg, Hagemann, Janoschka, Hager, & Schubert, 2016). These redox flow batteries are advantageous and one of the newer technologies that are capable of reserving production surplus to act as emergency backup power during unexpected conditions and times (Miyake & Tokuda, 2001). The following section provides brief categories of RFBs.

Zinc-bromine battery

The intermittence of energy generation from renewable energy sources has caused more attention to be focused on large-scale energy storage devices. Zinc–bromine battery is one of the redox flow batteries that have been designed and studied for large-scale applications. However, more studies need to focus on the up growth and reinforcement of Zinc-bromine RFB (Byrne & Macartain, 1999)

Zinc-bromine battery has been strongly established because of its superior high energy density, unlike other redox flow batteries. The electrochemical reaction shows that the Zn ion turns into zinc metal in the reduction process, while at the same time the bromide ion undergoes oxidation process and become bromine gas at the cathode during charging time (H. S. Yang, Park, Ra, Jin, & Yang, 2016). Unfortunately, electrochemical reaction of the zinc-bromine also causes the formation of poly-bromide at the negative electrode and deposition of zinc at the positive electrode during charging time, causing complication that may lead to decrease of energy efficiency, disrupted stability and durability of zinc-bromine electrolyte, crossover, lowering of coulombic efficiencies, and reduction of battery life (J. D. Jeon, Yang, Shim, Kim, & Yang, 2014; Kim & Jeon, 2015).

Studies have found that some additives may improve and recover zinc-bromine electrolyte conductivity as they enhance and boost the stability and durability of the electrolyte. Quaternary ammonium salts and dendrite inhibitors are some examples of additive which couple with energised bromine and directly inhibit the general formation of zinc dendrite. However, more studies about flow characteristic and behaviour are needed to increase stability, flexibility, and performance of the zinc-bromine RFB (H. S. Yang et al., 2016).

Iron-chromium battery

The first serious discussions and analyses of redox flow battery emerged during issues of unstable power distribution and iron-chromium RFB as the first RFB system appeared, employing Fe(II)/Fe(III) and Cr(II)/Cr(III) soluble redox couples as the anode and cathode active materials respectively, which are set apart by an ion exchange membrane as a separator and use carbon felts as the electrode material (Zeng, Zhou, An, Wei, & Zhao, 2016).

Iron–chromium redox flow batteries studies by (Fedkiw & Watts, 1984) have revealed these batteries as an auspicious energy storage system. However, a drawback of this flow battery is that it requires a catalyst to improve the electrochemical kinetics of the Cr(II)/Cr(III) redox reaction at the negative side. The chosen catalyst must have a high over potential towards the hydrogen evolution reaction; because these reactions may reduce columbic efficiency and cause an imbalanced state of charge (SOC) that leads to capacity decay. Some catalysts like Au-Ti and Bi are deposited on the electrode surface and lighten the process. Yet, there is a problem that needs to be tackled; this flow battery is different from other flow batteries because the membrane of iron–chromium battery is permeable both to charge carrier ion(H^+/Cl^-) and active species (Fe/Cr) (Zeng, Zhao, An, Zhou, & Wei, 2015). This phenomenon will form a large concentration difference through the membrane and cause a high crossover rate effect.

Bromide- polysuphide

Bromine–polysulphide battery is a flow battery that comprises sodium bromide at the positive electrolyte and sodium polysulphide on the negative side. Bromine–polysulphide battery was patented by Remick and further studied by Regenesys technologies since 1993s (Weber et al., 2011). This flow battery has been favoured for commercialisation for redox flow technologies since 1993s until 2003s due to its good characteristics and significance by having a moderate cost and being highly soluble in aqueous solution without implementing any catalyst to speed up the reaction.

Studies on bromine–polysulphide batteries have shown the unique features of this energy storage system which are the abundance of the two electrolytes, reasonably inexpensive cost, and high solubility in aqueous solution. However, the disadvantages of this flow battery are complex electrode reaction, the risk of cross-contamination and need to be fully monitored (Denholm et al., 2010). This flow cell also releases heat and toxic gases which are not environmentally friendly, thus calling for new action and plan for future implementations of bromine–polysulphide flow battery.

Vanadium RFB (V-RFB)

Works on Vanadium Redox Flow Battery (V-RFB) technology was spearheaded by Maria Skyllas-Kazacos and her colleagues at the University of New South Wales (UNSW), Australia in the 1980s (Parasuraman et al., 2013). The Kazacos research team has revealed and shown that this battery has many unique features and characteristics compared to other conventional batteries. V-RFB is already commercialised in Japan by Sumitomo Electric Industries (SEI) and has already been tested and practised in Tottori Sanyo Electric (Fisher et al., 2014). However, the research and development of V-RFB are continuing until today to suit the demands of technologies and for more practicalities in various applications. There is a large volume of published studies describing the fundamentals and proposition of V-RFB system. A standard structure of V-RFB reserves energy in two separate liquids involving the same redox couples and the same metal ions in both half-cells. Here, vanadium ions are used at the coupled positive and negative electrodes through the membrane V(II)/V(III) redox couple is active at the anode side while the cathode side uses the V(IV)/V(V) redox couple (Huang, Li, Liu, Tan, & Chen, 2008). The system also consists of two pumps, electrodes, flow frames, bipolar plate, and ion exchange membrane (Blanc et al., 2008).

During the charging stage, hydrogen ions (H+) are initially at the positive side and move to the other side through the exchange membrane and vice versa during the discharging moment. The balance in the electric charge is obtained by the transfer of hydrogen ions beyond a membrane that functions to separate the electrolytes (Ponce de

León et al., 2006). Among various energy storage technologies, V-RFB appears promising because of its supreme features such as effective and simple operation, capability of high power, operationally at room temperature, fast speed response and recharging contenders, excellent chemical stability that shows an extremely long-round-trip cycle, long discharge times, and good modular design (Alotto et al., 2012). V-RFB also exhibits for highly reversible redox kinetics, has been developed for large-scale applications and has reasonable and controlled maintenance cost compared to conventional batteries (Hopkins, Smith, Slocum, & Chiang, 2015). The unique feature of V-RFB is that it has decoupled energy storage and power component that give independent control of capacity and power (Rusllim Mohammad et al., 2010). V-RFB has become the most attractive battery for EV applications on target for vehicle configuration especially for optimisation of power and energy.

V-RFB cells may be constructed in a series or parallel arrangement (Zhao et al., 2006). In the past 20 years, V-RFB has been one of the major projects for commercialisation and industrialisation (Parasuraman et al., 2013). Furthermore, V-RFB performance has been extended and prolonged by focusing more on the invention on new novel electrode materials, catalyst on different substrates, enhancement on electrolytes to increase energy density, ion exchange membranes and additives, and optimisation of the system that included a battery cell/stack on the structure and operating conditions (Jyothi Latha & Jayanti, 2014b). In addition, there is no risk of hydrogen explosion hazard due to technically good charging and discharging processes without harming the battery (Skyllas-Kazacos, Chakrabarti, Hajimolana, Mjalli, & Saleem, 2011). Despite many interesting studies indicating the potential of V-RFB have been reported before, the V-RFB development system remains to be further explored. The many potential benefits of V-RFB makes this battery is chosen rather than other batteries for this study.

2.7 Key components of V- RFB

Figure 2.1 represent the components of V-RFB cell to become one complete cell stack. The main parts of a unit cell of V-RFB, which consist of cell membrane, flow frame electrode (cell geometry) and pumping system. V-RFB basically comprises of positive and negative parts containing an anolyte and catholyte with an interposed membrane or ionic separator. So, one-unit cell stack consist of two half-cell is separated by a membrane. V-RFB store energy in two electrolytic solutions containing redox couples.

The solutions are circulated through their external tanks by means of two pumps. Similarly, to fuel cell this architecture decouples power rating, which depends on the stack size, from stored-energy rating, which depends on the tanks volume. The overall stack structure is shown in Figure 2.2. Next, a multiple cell can be stacked together in series to produce a modular stack as illustrated in Figure 2.3.

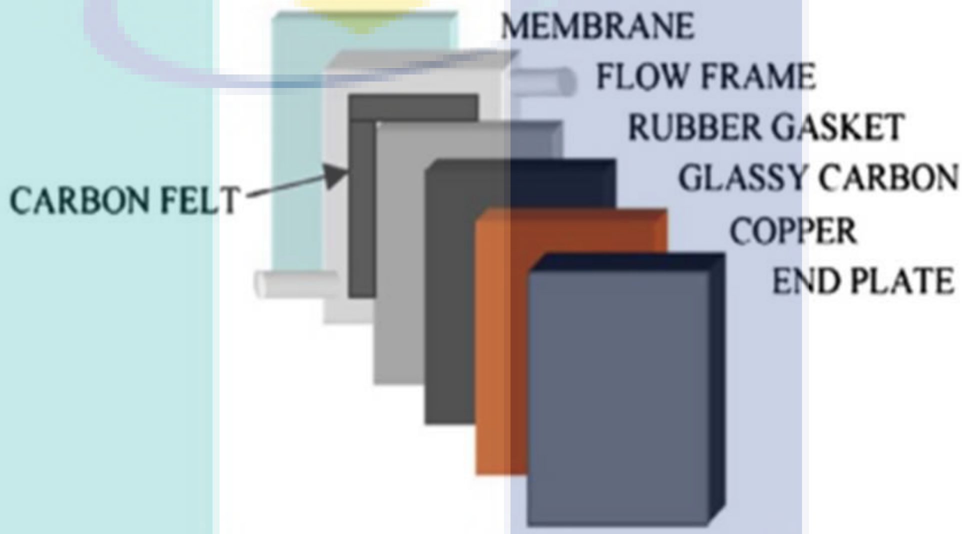

Figure 2.1 Components of V-RFB cell stack

Source: (Parasuraman et al., 2013)

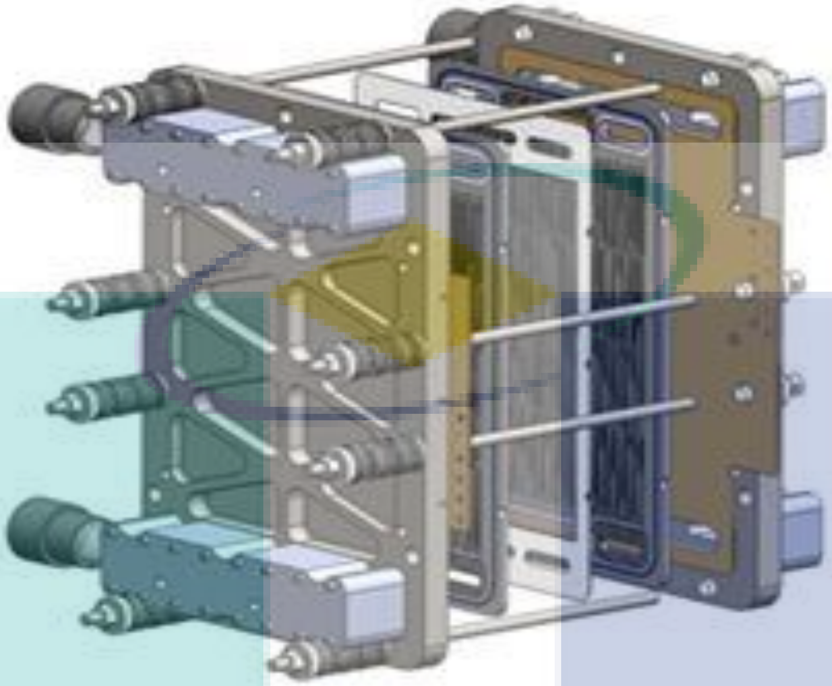

Figure 2.2 Complete single unit of V-RFB cell
Source: (Fisher et al., 2014)

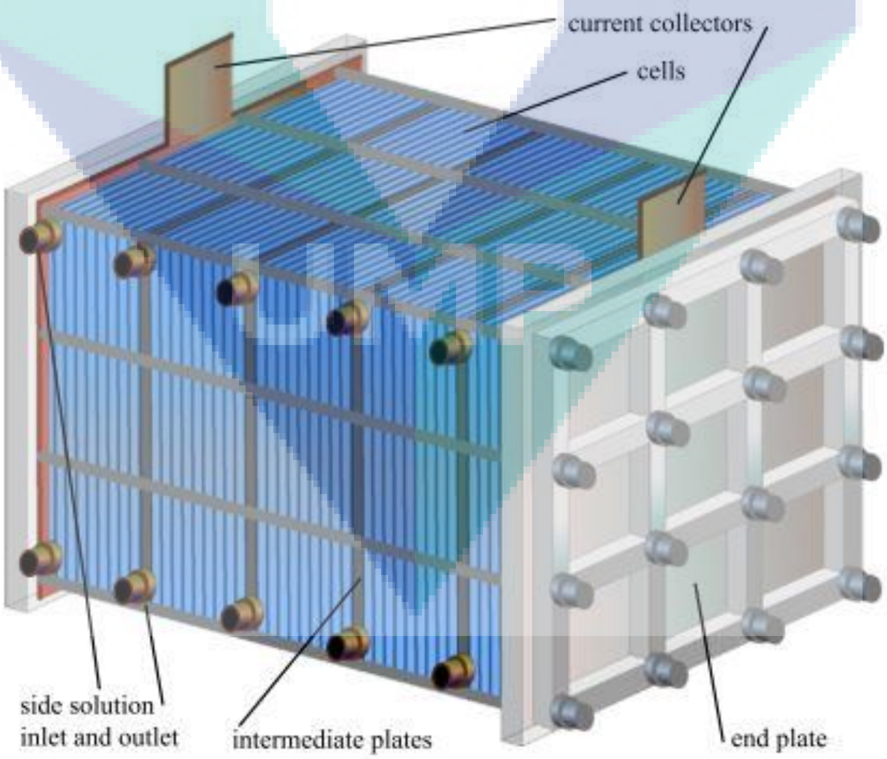

Figure 2.3 Modular stack
Source: (Alotto et al., 2014)

Electrode material (cell geometry)

The electrode material contributes a significant impact on the redox reaction in the electrochemistry of V-RFB. The electrode is porous and made from a carbon-based material, such as carbon felt, and graphite felt. The electrode material is easily corroded due to CO2 evolution. CO2 evolution leads to battery failure and directly lowers its energy efficiency (Liu, Xu, Yan, & Qiao, 2011). Carbon-based material is an excellent V-RFB electrode material because of its three-dimensional network structures and has wide operating potential range, good electrical and chemical conductivity and stability, relative inertness, acid resistance, and long cycle life in an acidic environment (Chakrabarti et al., 2014). Unsuitable design of electrode material (cell geometry) could make the flow of the electrolyte non-uniform. Uneven flow distribution may result in non-uniform current distribution, with the possibility of locally overcharging causing gas evolution and degradation of the bipolar plates (Bhattarai et al., 2017). Therefore, more developers and researchers are at pains to design the cell geometry to ensure even distribution of the electrolyte through the porous electrode. Hence, most suitable electrode material in anode and cathode half-cells design in vanadium flow battery is selected to enhance the electrochemistry activities and maintain mechanical integrity (Parasuraman et al., 2013).

Membrane (ionic separator)

There are three main components for the V-RFB storage system. One of the main components is an ion exchange membrane or called separator. The separator's role is to passage the ion between the positive (catholyte) and negative (anolyte) sites while prohibiting the crossover of the electrolytes during the transfer of current (D. Chen et al., 2013). The membrane normally used in the flow battery is from perfluorosulfonic acid polymer like DuPont's Nafion membrane (Wu et al., 2014). To improve the performance and energy efficiencies of the V-RFB, a high-quality membrane has been the focus for development in V-RFB system. The criteria for selecting a good and ideal membrane are listed as follows (Fujimoto et al., 2014; Parasuraman et al., 2013):

I. Good membrane durability to enhance oxidation resistance and good ionic exchange capacity.
II. High ionic conductivity and good chemical stability under strong acidic environment.
III. High permeability to the charge-carrying ions & excellent thermal stability.

The unit cell and modular stack

This unit cell of V-RFB cell comprises a bipolar electrode which is electrically conductive carbon-composite material, an ion-exchange membrane which acts as a separator between two electrode layers in anion and cation electrodes, and a non-conductive plastic as the frame as shown in Figure 2.4. This complete single unit of the battery cell is connected together with positive and negative tanks that store the active material, pump, and piping for the circulation of electrolyte from the tanks to the battery cell (Shigematsu, 2011). V-RFB stacks are built from individual or single unit cells which are stacked in series or parallel. This single unit are assembled to form a V-RFB stack. A multi-layer structure of cells in which the electrochemical reaction occurs is called a cell stack (Shibata, Kumamoto, Nagaoka, & Kawase, 2009). Figure 2.4 present the configuration of a single unit, cell stack, and V-RFB system.

This cell stack is constructed with flow frame's cavity flow for pathways of electrolyte for absorbent activities in carbon felts that are inserted into the flow frames. Every single cell contains a location or marks the spot where the chemical charge transfer reaction occurs (Weber et al., 2011). The performance of a RFB system is highly dependent on cell materials, cell design, stack design, and electrolytes (Fisher et al., 2014). A single unit can be arranged in two manners: unit cell fed by electrolyte in parallel or arranged in series, where all the modules operate with the same inlet with a stack arranged in parallel or the modules are connected hydraulically in a series, and the electrolytes flow successively through each of them (Arenas et al., 2017).

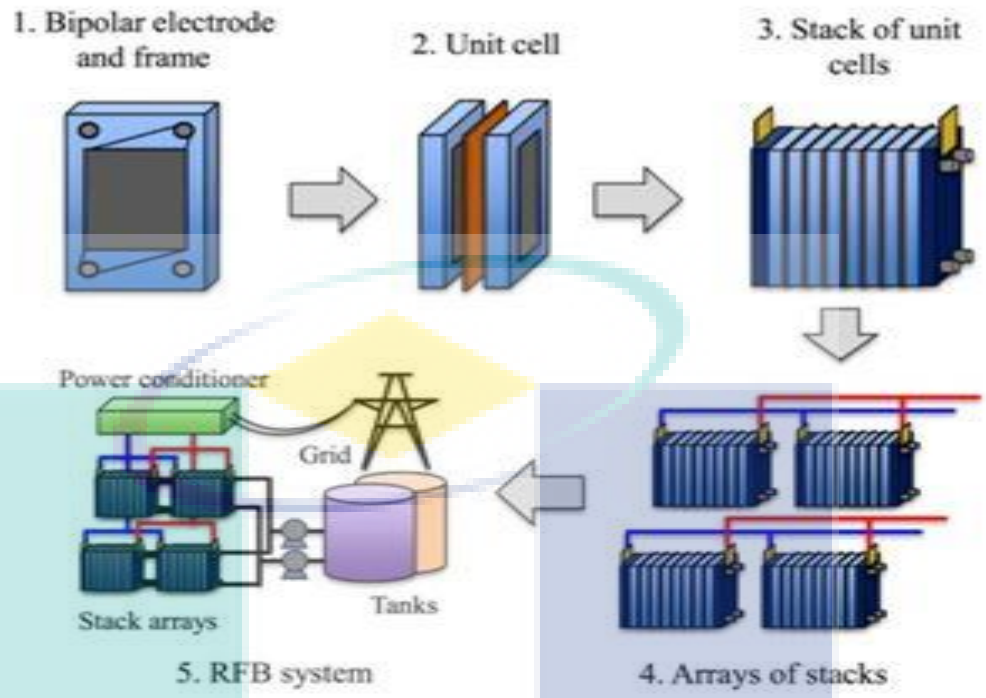

Figure 2.4 Configuration of single unit, modular stack and complete battery system of V-RFB

2.8 V-RFB cell features and design

V-RFB cell design, first patented by Skyllas-Kazacos and team in 1988s (Rychcik & Skyllas-Kazacos, 1988). An historical overlook of early RFBs pattern is followed and inspired by a report of (Thaller, 1976). Ever since, various publications emerge for redox couples (P. K. Leung et al., 2015), material properties (Seyed Schwan Hosseiny, 2011) and cell design (Aaron et al., 2012). However, the studies on the cell design for V-RFB remain limited. Hence, the key issue associated with the flow geometry design is improvising to get an optimal design and operating conditions for V-RFB system.

Cell geometries design (electrode compartment)

One of the most significant current discussions in the optimisation of V-RFB is on cell design and architecture of flow stack battery system. The cell geometry is one of the crucial parts for determining flow distribution of liquid and mass transport within the cell. Good cell geometry designs exhibit uniform electrolyte distribution to the entire surface of the electrode and leading to minimize pump power consumption of the cell, which is one of the key requirements for energy storage technologies. Cell geometry aspect correlation is also important (Houser, Pezeshki, Clement, Aaron, & Mench, 2017). It is interesting to note that currently, new and flexible cell geometries are being studied and redesigned by previous researchers as an alternative to replace the conventional one for optimisation. (A. C. Khor et al., 2016) proposed rhombus cell geometry as an alternative design for use in V-RFB system instead of the conventional square design. The study found that rhombus cell geometry exhibited the best uniformity of electrolyte in the cell and showed the lowest pressure drop compared to conventional square design. Nevertheless, the studies implemented only on one flow pattern and are concluded in general terms and no specific data result on the overall pump power required of V-RFB with a proposed cell design.

(Xu, Zhao, & Leung, 2013) proposed no flow, parallel and serpentine flow channel pattern while maintaining a traditional square shaped. (Jyothi Latha & Jayanti, 2014b) present comparative studies with various flow channel pattern which were plain, parallel, serpentine and an interdigitated design, exhibits a new flow channel pattern but same as previous work by maintaining a traditional square cell shaped. All this work claimed that by adding a flow channel pattern is much better and successfully minimizing pump power consumption needed by V-RFB system. However, studies mostly focused on flow channel design, thickness of electrode, and different positions of inlet/outlet channel while maintaining square cell geometry because the focus is more on the characterisation of V-RFB, and not cell and architecture design development (Alotto et al., 2014; Mohamed et al., 2015a). It should be noted that electrochemical cell geometry has not been well studied and deeply discussed.

Therefore, this calls into question whether this flow cell design is optimum to be applied or if other geometries may lead to a more efficient flow battery cell, because different cell configurations may have different electrolyte distributions (Bortolin, Toninelli, Maggiolo, Guarnieri, & Del Col, 2015). An exhaustive review of these studies has suggested a direction for future development and lead to the motivation to study alternative cell geometries with a various flow channel to enhance flow distribution, minimise the pump power within the cell, and improve the performance of the flow battery.

Flow channel pattern

The cell geometries are designed with precise flow channels that will direct the electrolyte to flow through the entire area of electrode evenly and completely. Studies on flow channel development aim to develop better electrolytes on the electroactive site compartment and strengthen the structure for electrode material (Xu et al., 2013). Figure 2.5 shows the complete schematic of a battery system with/without flow channel to study the flow behaviour in the cell. By applying a good flow channel, the pump loss would be lessened and may improve and stabilise the uniformity of concentration distribution, and enhance mass transport due to good convection and diffusion of electrolytes (Bortolin et al., 2015; X. You, Ye, & Cheng, 2016).

(Xu, Zhao, & Zhang, 2014a) have reported their experimental and numerical investigations concerning RFB. They studied the performance of V-RFB with and without a flow field (flow channel) by carrying out the experiment while at the same time numerically designing a three-dimensional model to study the flow field design for the flow battery. Results from experimental work showed that energy efficiency of V-RFB is much higher (around 5%) when electroactive sites of the flow field are applied compared to energy efficiency without the flow field. Therefore, the conclusion here is that a flow field channel in V-RFB improves system efficiency of the battery. The numerical work result showed that there is a uniform distribution of electrolytes over the entire active area of the electrode surface when a flow field channel is applied. A cell with a flow field has a more significant reduction in the pressure drop, especially with the parallel design.

(Tüber, Oedegaard, Hermann, & Hebling, 2004), proved that pressure drop is not the only criterion that needs to be investigated; the reactant transportation through the reaction sites also needs to be included. They also claimed that the design of flow channel for V-RFBs is an important area that needs more investigation and as there is not much literature on the subject. (Bhattarai et al., 2017) proposed four types of electroactive flow channels: rectangular open channel, interdigitated open cut channel, interdigitated circular poked channel, and cross poked circular channels. All four types were compared to the conventional channel. In the study, using a flow channel improved the overall battery performance. However, there is limited information about the effect of different types of channel from the literature.

Numerical and experimental studies of flow channel and flow distribution effects in V-RFB have also shown that a flow channel design would be advantageous for large-scale systems and suitable flow channel configuration designs may give significant differences on the performance and uniformity of flow batteries (D. H. Jeon, Greenway, Shimpalee, & Zee, 2008).

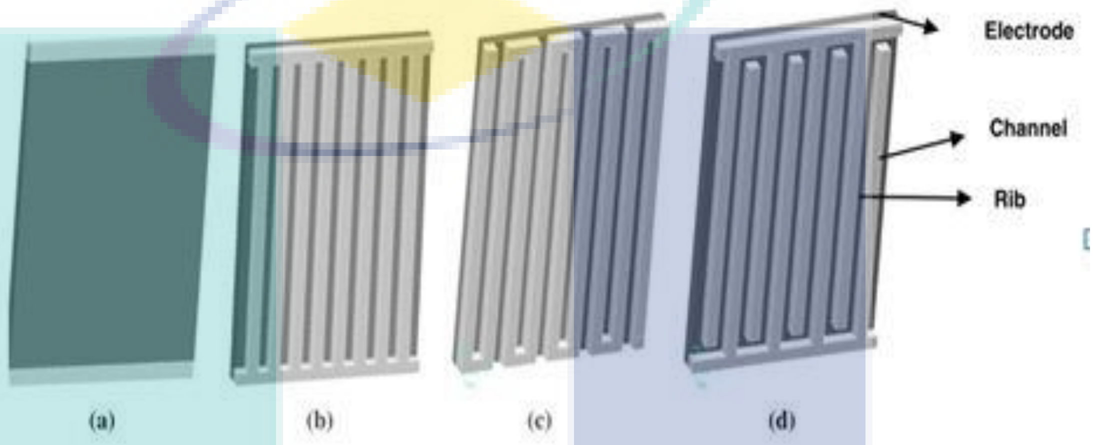

Figure 2.5 Schematic of a battery system with/without flow channel a without flow channel, b parallel, c serpentine, d interdigitated

Pressure drop and pump power effect within the cell geometries design

The pressure drop in V-RFB cell geometries is the most important indicator to ensure the suitability of the cell geometries, as indicated by the lesser pressure drop required with optimum flow rates within the cells. More pressure drop losses are in between the stack, manifolds, and channel, so there is a significant relationship of pressure drop losses with the battery system which needs to be focused on for continuous circulation of the electrolytes through the cell, based on the suitable flow rates applied (Jyothi Latha & Jayanti, 2014a). Then, pump energy consumptions (pump power) is dependent on the pressure drop; the higher the pressure drop within the cell, the higher the pump energy consumption in V-RFB system (Brown et al., 2016). Researchers have revealed that high pressure drop consumes excessive pumping energy that may lead to lower system efficiency (Xu et al., 2013).

This high pressure drop factor is related with improper flow frame cell geometries, which tend to give lack of good control in a real behaviour system and may restrain battery performance (Yin et al., 2014).

2.9 Scale-up system

There are few researches that focus on the engineering aspect of design, cell construction, and scale-up progress. Several studies have revealed that one of the limitations of this green energy storage system is unsuccessful scale-up, poor maintenance, the high cost of development, and low efficiency (Perry & Weber, 2016). So, the consideration of the effect of cell design, electrode structure, and operational conditions need to be focused on to overcome these problems. This is supported by a study which highlighted on the design of energy storage system and scaling up work for a better adoption for these battery technologies (Arenas et al., 2017).

Scaling up lead to an efficient system and less cost consumed for device commercialisation. Scale-up may be performed through parametric studies (current density, electrolyte flow rate, linear velocity and electrode size, mass transport, and dimensionless group), modelling, and simulation, and these studies enable researchers to better understand the complex work and relationship between performances (Cervantes-Alcala & Miranda-Hernandez, 2018). Dimensional analysis that includes electrode geometry, reaction kinetic and fluid flow is also included in the process and stages on the development of scale-up works. Thus, the design and scale-up of these devices have to take such relationships into account. The V-RFB flow cell battery is tested in a laboratory or simulated as a single unit cell and then scaled-up to a pilot stack, which are designed by taking into account the effects of the electrolyte flow regime. This pilot stack should be easy to modify and test to control another operating parameter such as shunt current, electrode potentials, and pressure drop (Arenas et al., 2017).

There is a research by (Rusllim Mohammad et al., 2010) that estimated the size of scaled-up and performance of a series of electric vehicles that use V-RFB. However, the case study did not provide enough numerical investigation or any experimental work evident to support the scaled-up size result. Therefore, this became a motivation for this work to study the scale-up progress for V-RFB system in terms of parametric studies.

2.10 Parameter estimation

To fit an equivalent circuit model to a specific battery cell, parameter estimation is a common process to go through (Jackey et al., 2013). It is also to identify sources of error and discrepancy. To implement parameter estimation, analyse the measured current data to locate the exact pulse transitions, remove noise by filtering the raw data, set the initial values for the equivalent circuit elements, for circuit lookup table the exact State of Charge (SOC) is calculate, the settings for the optimization algorithm need to be choose and gauge, and a series of estimations is perform to determine the optimum parameters (Jackey et al., 2013; Z. Zhang, 1997). Almost all of parameter estimations depend on the applications or design produced error. There are many methods of parameter estimation for example artificial neural network (ANN), spline techniques, linear parameter varying, change current, and Extended Kalman Filter (EKF). Table 2.2 shows parameter estimation methods.

Table 2.2 Comparison of parameter estimation methods

Methods	Advantages	**Disadvantages**
Artificial Neural Network (ANN); can be used for pattern extraction or complex trend that are hard to be noted by computer or human.	Can transform complicated and precise date to meaning derivation.	Input and output dataset hard to identify
Spline technique; piece wise polynomial of degree 'n'	Easy to handle because of simple polynomials Good for the behaviour of actual system	Overshooting occur at high polynomials degree at intermediate point

Current change; simple technique that changes the output current to obtain the transient waveform at the terminal voltage	Can be used to get accurate quantitative result and quick qualitative indication not a problem for the current change method to perform for single, small, and even larger stack of battery	changes in load current causing related voltage to change
Extended Kalman Filter (EKF); common application of Kalman Filter	Minimize system error Can gauge parameter data accordingly which can save time Low cost	

2.10.1 Extended Kalman Filter (EKF)

EKF is the common application of Kalman Filter (KF) in a nonlinear system and one of the best estimators from noisy data amount to filter out the noise. It is also very convenient for real-time processing and is quite straight forward to be implemented if a priori information of the measurement and process noise covariance matrices are available (Banani, 2007; Caiping Zhang, Jiang, Zhang, & Sharkh, 2012). EKF linearized nonlinear model to linear model (Banani, 2007; Grewal & Andrews, 2001; Kleeman, 1996; M. R. Mohamed et al., 2013). By reducing the state covariance, it can minimize the estimation error. EKF can measure data even though the data is full of infected noise.

2.11 Chapter conclusion

In this chapter, review of literature is given emphasis and some studies were used as a guide to complete this project. RFB was chosen due to low maintenance, fast response time, and longer lifespan. V-RFB was used for this project because it had a lesser chance for cross-contamination, the battery would not be affected for overly discharged, and high energy density.

V-RFB system beats the advantages and performance of other reliable energy storage technologies such as flywheel, PHES, CAES, and other conventional batteries due to its flexible battery design which offers independent power and energy capabilities and a long-life cycle. V-RFB system also uses the same element for the positive and negative active materials, thus reducing the risk of cross contamination that may otherwise lead to poor performance.

This chapter provides a relevant and clear understanding on how the different cell geometries and flow channel designs influence the pump energy consumption (pump power) and electrolyte distribution. Based on the brief review, optimisation of V-RFB needs continuous efforts, especially on the development of cell design, which is a key component of V-RFB.

The equivalent electrical circuit model was chosen to represent V-RFB because of easy to derive, simulate and also less complex. To adequate proposed equivalent circuit into V-RFB, parameter estimation took place by using EKF which can measure data accordingly and also can save time.

CHAPTER 3

METHODOLODY

3.1 Chapter overview

This chapter explains the research methodology on equivalent circuit model for V-RFB. For equivalent circuit model, it has two types actual and approximate. Construction of equivalent circuit model are presented along with method and software used for parameter estimation.

3.2 Project review

Based on the project, research about the related project has been conducted. Every related article or journal has been through to find the best methods that will be used in this project. The methods used for this project will be following the flow chart below. Figure 3.1 below displays the project flow from the beginning to the end of the project.

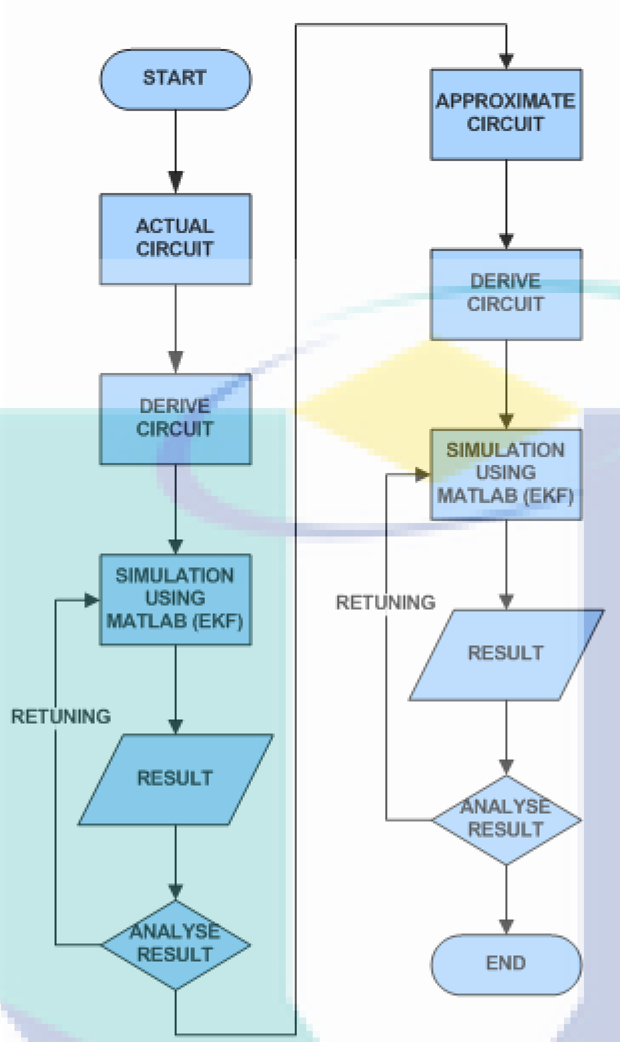

Figure 3.1 Flow chart of project methodology

Equivalent electric circuit models for V-RFB was proposed which consist of actual and approximate circuit. From actual circuit, the circuit was derive thoroughly and from the derivation recursive EKF algorithm was construct. Simulation using EKF method in MATLAB software take place to estimate each parameter of both actual and approximate circuit. Based on the result through the simulation, if the expected result are not achieved, the simulation will be continuously retuning to obtain better result.

3.3 Modelling

Equivalent electrical circuit has widely been researched and used due to its simplicity and adaptability on any circuitry design system. The connection at the battery terminal between voltage and current is known as an electric circuit. The proposed equivalent electrical circuit for V-RFB resembles (Choi, Enjeti, & Howze, 2004) and (Chang, 2013). Both researchers used the circuit for Fuel Cell (FC) (Chang, 2013) to estimate parameter of the circuit for FC using current change method, whereas (Choi et al., 2004) used it to evaluate current ripple effect for Power Conditioning Unit (PCU). FC and RFB are similar theoretically. However, in the FC system the electrolyte remains in the cell stack, whereas in RFB redox reaction occurs as the electrolyte flows through the cell stack. The equivalent circuit is also proposed based on the design consideration in (Salerno & Korsunsky, 1998) with the present of parasitic inductance. Parasitic or stray inductance is an unintended inductance in a circuit and has undesired effect in a way. However, in some applications parasitic inductance give desired effect; helical resonators and battery protection circuit. Equivalent circuit model presented has two types actual and approximate.

Actual circuit

Equivalent electrical circuit in Figure 3.2 contains of an open circuit cell potential, $E_{cell(orp)}$ that signifies the SOC and temperature of the V-RFB, an internal ohmic resistance, R_o that corresponds to the effect of current excitation, inductor for battery performance, X_L the polarization resistance is R_{a1}, R_{a2}, R_{c1}, R_{c2}, and R_m, where R_{a1} and R_{a2} represent effective resistance describing activation polarization, R_{c1} and R_{c2} represent effective resistance describing concentration polarization, Rm for mass transfer resistance; while C_a, C_c, and C_m represent effective capacitance parameters. Compare to Figure 2.2, Figure 3.2 has additional resistors and capacitors for activation, concentration, and mass transport polarization and also an inductor for battery performance.

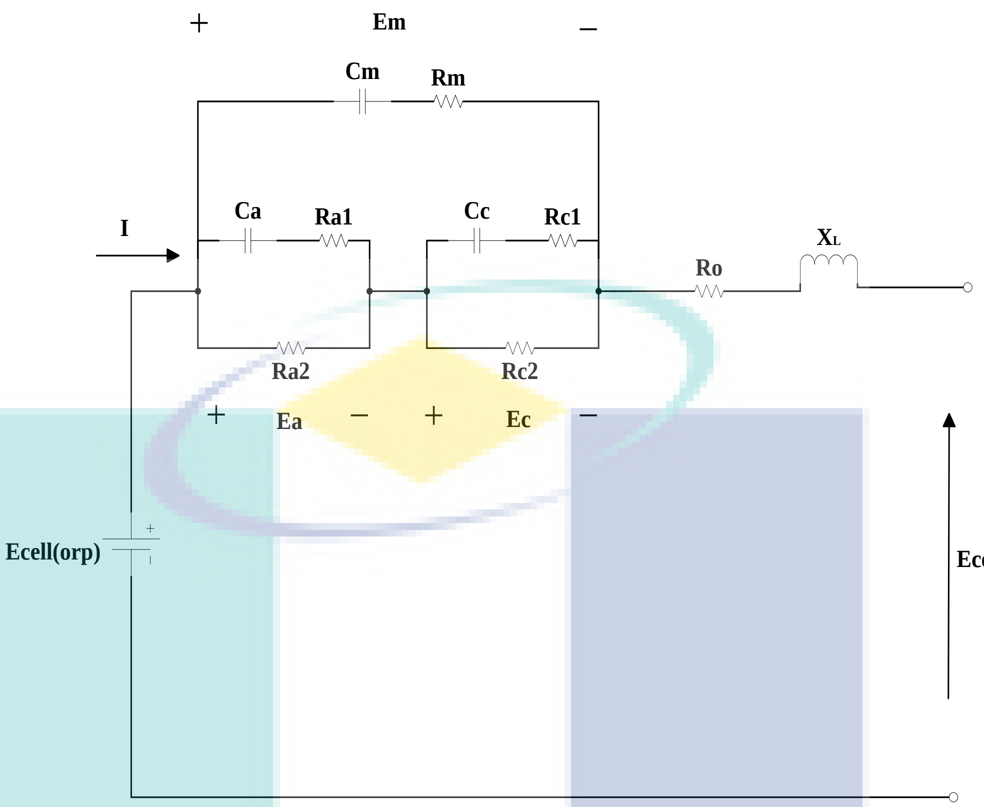

Figure 3.2 Actual circuit for V-RFB system

This part describe modelling equation for proposed circuit. The electrical behaviour of the actual circuit can be stated by applying Kirchhoff's Voltage Law (KVL):

$$E_{cell} = E_{cell(orp)} - I(X_L + R_o) - E_m - E_a - E_c \tag{3.1}$$

The ordinary differential equation across the polarizations is:

$$E_m = \frac{I}{C_m + R_m} - \frac{E_m}{(C_m + R_m)(C_a + R_{a1} + C_c + R_{c1})} \tag{3.2}$$

$$E_a = \frac{I}{C_a + R_{a1}} - \frac{E_a}{C_a R_{a2} + R_{a1} R_{a2}} \tag{3.3}$$

$$E_c = \frac{I}{C_c + R_{c1}} - \frac{E_c}{C_c R_{c2} + R_{c1} R_{c2}} \tag{3.4}$$

State variables of V-RFB

$$E_{cell} = -\left[\frac{1}{C_m + R_m} + \frac{1}{C_a + R_{a1}} + \frac{1}{C_c + R_{c1}} + \frac{L}{C_c R_{c2} + R_{c1} R_{c2}}\right] I + \left[\frac{1}{(C_m + R_m)(C_a + R_{a1} + C_c + R_{c1})} - \frac{1}{C_c R_{c2} + R_{c1} R_{c2}}\right] E_m + \left[\frac{1}{C_a R_{a2} + R_{a1} R_{a1}} - \frac{1}{C_c R_{c2} + R_{c1} R_{c2}}\right] E_a + \left[\frac{1}{C_c R_{c2} + R_{c1} R_{c2}}\right] E_{cell(orp)} - \left[\frac{1}{C_c R_{c2} + R_{c1} R_{c2}}\right] E_{cell} \quad 3.5$$

Approximate circuit

Equivalent electrical circuit of V-RFB shown in Figure 3.2 has a potential to approximate some of the parameters which can be lumped together for a simpler circuit due to complexity in representing the simulation results. Figure 3.3 shows the approximate equivalent circuit for V-RFB. It also consists of an open circuit cell potential, $E_{cell(orp)}$, an internal ohmic resistance, Ro and inductor, X_L which as impedance of inductance (Z_L) same as circuit shown in Figure 1, impedance of mass transfer, Z_m (C_m and R_m), and a pair of Resistor-Capacitor (RC) branches that represent the time-dependent V-RFB's dynamics of activation, Z_a (C_a, R_{a1} and R_{a2}) and concentration, Z_c (C_c, R_{c1} and R_{c2}) polarizations. Overall, the polarization in the circuit shown in Figure 3.2 and 3.3 are used to describe the transient response at power transferring of the battery.

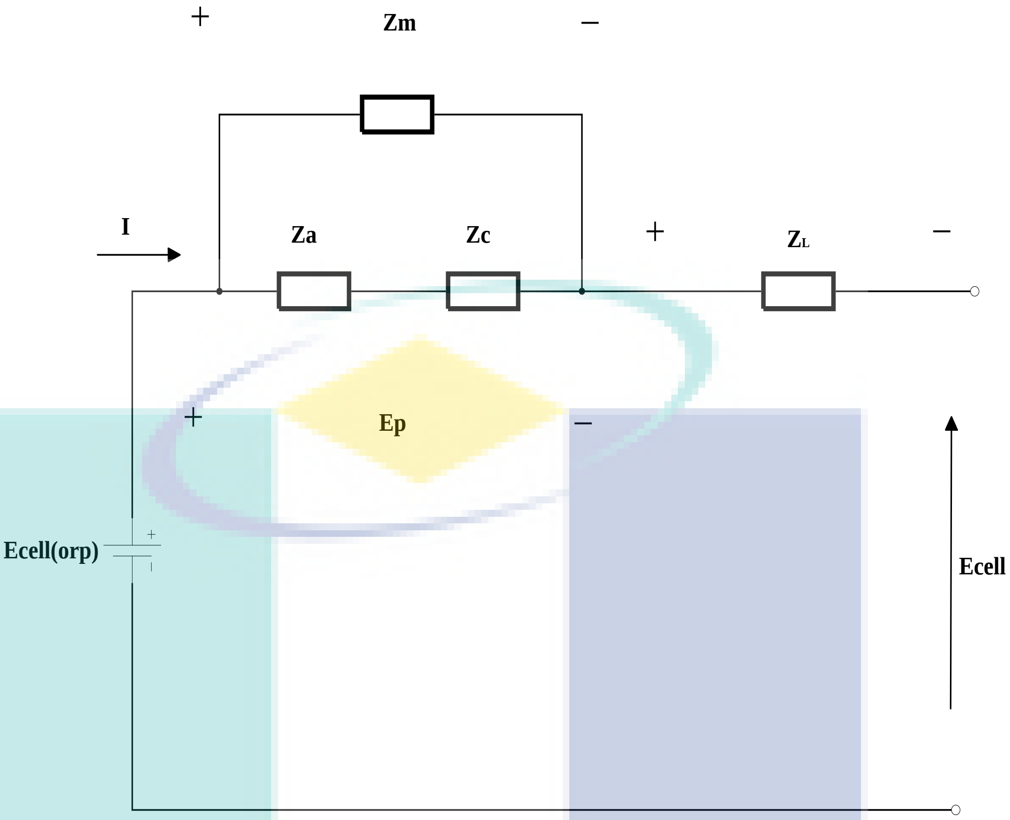

Figure 3.3 Approximate circuit of V-RFB

The following equation is the expression of the approximate circuit:

$$E_{cell} = E_{cell(orp)} - E_p - IZ_L \qquad 3.6$$

The ordinary differential equation across the polarization is:

$$\dot{E_p} = \frac{I}{Z_m} - \frac{E_p}{Z_m(Z_a + Z_c)} \qquad 3.7$$

State variables of V-RFB:

$$\dot{E_{cell}} = -\left[\frac{1}{Z_m} + Z_L\right] + \left[\frac{1}{(Z_a+Z_c)Z_m}\right] E_p + E_{cell(orp)} \; - E_{cell} \qquad 3.8$$

3.4 Parameter estimation

EKF is the common application of Kalman Filter (KF) in nonlinear system and one of the best estimators from noisy data amount to filter out the noise. It is also very convenient for real-time processing and is quite straight forward to be implemented if a priori information of the measurement and process noise covariance matrices are available (Banani, 2007). EKF in MATLAB was used to estimate parameters of the proposed electrical circuit for V-RFB. EKF linearized nonlinear model to linear model. By reducing the state covariance it can minimize the estimation error. Clarification of continuous-time with discrete-time measurement are per below (He, Xiong, Zhang, Sun, & Fan, 2011):

$$\left.\begin{array}{c} x_k = f_k(x_{k-1}, u_k, w_k \\ z_k = h_k(x_k, v_k) \\ w_k \sim (0, Q_k) \\ v_k \sim (0, R_k) \end{array}\right\} \qquad 3.9$$

System output current is u_k, the process noise in continuous-time Gaussian zero mean white noise with covariance of Q_k is w_k whereas the measurement noise in discrete-time Gaussian zero mean noise with covariance R_k is v_k. Figure 3.4 the operation of EKF in estimating optimal or quasi-optimal value of V-RFB parameters.

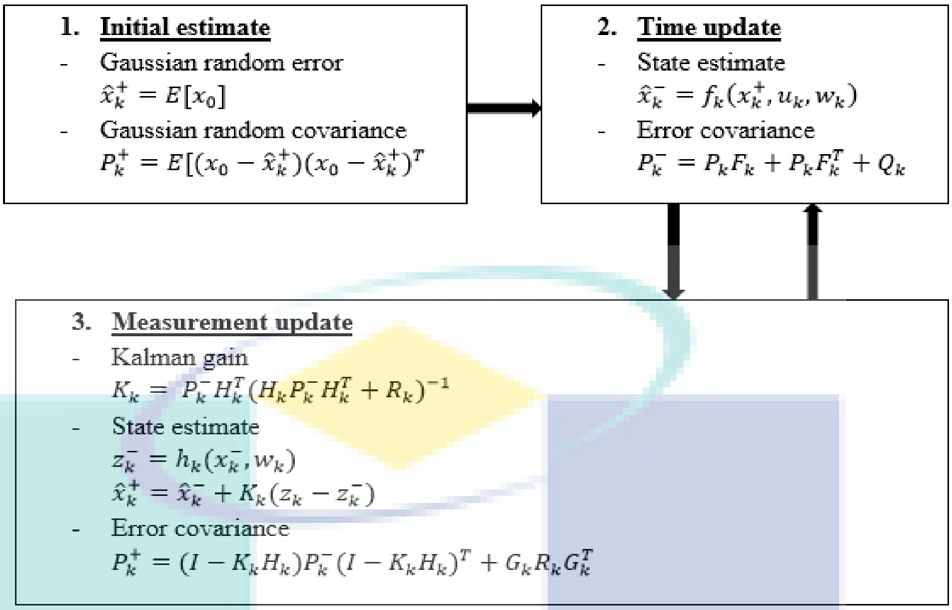

Figure 3.4 Implementation flowchart of EKF algorithm in estimating optimal or quasi-optimal of V-RFB parameters.

EKF of actual circuit for V-RFB

Form of (3.9) is used to illustrate state variable of the parameter of actual circuit for V-RFB by applying equations (3.2), (3.3), (3.4) and (3.5) for model development. State x_k as:

$$x_k = [E_m \ \ E_a \ \ E_c \ \ E_{cell} \ \ R_m \ \ C_m \ \ R_{a1} \ \ R_{a2} \ \ C_a \ \ R_{c1} \ \ R_{c2} \ \ C_c \ \ Z_L]^T \qquad 3.10$$

From state model with deliberation of input variable:

$$f(x_k, u_k) = [f_1 \ \ f_2 \ \ f_3 \ \ f_4 \ \ f_5 \ \ f_6 \ \ f_7 \ \ f_8 \ \ f_9 \ \ f_{10} \ \ f_{11} \ \ f_{12} \ \ f_{13}]^T \qquad 3.11$$

$$z_k = h_k(x_k) = [0 \quad 0 \quad 0 \quad E_{cellk} \quad 0 \quad 0 \quad 0 \quad 0 \quad 0 \quad 0 \quad 0 \quad 0 \quad 0]^T \qquad 3.12$$

Where$u_k = I$, $f$is the transition matrix of V-RFB system, and h_k is measurement matrix. Thus, $f_s(s = 1, 2, 3, 4, 5, 6, 7, 8, 9, 10, 11, 12, 13)$ are describe as:

From (3.2), $f_1 = -x_1/(x_6 + x_7)(x_9 + x_7 + x_{12} + x_{10}) + (x_6 + x_5)u_k$

From (3.3), $f_2 = -x_2/(x_8 (x_9 + x_7)) + (x_9 + x_7)u_k$

From (3.4), $f_3 = -x_3/(x_{11} (x_{12} + x_{10})) + (x_{12}+x_{10})u_k$

From (3.5), $f_4 = -x_4/(x_{11} (x_{12} + x_{10})) + x_2 ((1/(x_8 (x_9 + x_7))) - (1/(x_{11} (x_{12} + x_{10}))) + x_1 ((1/(x_6 + x_5)(x_9 + x_7 + x_{12} + x_{10})) - (1/(x_{11} (x_{12} + x_{10})))) - ((x_6 + x_5) + (x_9 + x_7) + (x_{12} + x_{10}) + (x_{13}/(x_{11} (x_{12} + x_{10})))) uk + E_{cell(orp)} /(x_{11} (x_{12} + x_{10}))$

Thus, $f_5 = f_6 = f_7 = f_8 = f_9 = f_{10} = f_{11} = f_{12} = f_{13} = 0$ 3.13

From (3.15) the matrix representation of the model, F is calculated as:

$$F = \frac{\partial f}{\partial x} | x = \hat{x}$$

$$= \begin{bmatrix} a_{11} & 0 & 0 & 0 & a_{15} & a_{16} & 0 & 0 & 0 & 0 & 0 & 0 & 0 \\ 0 & a_{22} & 0 & 0 & 0 & 0 & a_{27} & a_{28} & a_{29} & 0 & 0 & 0 & 0 \\ 0 & 0 & a_{33} & 0 & 0 & 0 & 0 & 0 & 0 & a_{3,10} & a_{3,11} & a_{3,12} & 0 \\ a_{41} & 0 & 0 & a_{44} & a_{45} & a_{46} & a_{47} & a_{48} & a_{49} & a_{4,10} & a_{4,11} & a_{4,12} & a_{4,13} \\ 0 & 0 & 0 & 0 & 0 & 0 & 0 & 0 & 0 & 0 & 0 & 0 & 0 \\ 0 & 0 & 0 & 0 & 0 & 0 & 0 & 0 & 0 & 0 & 0 & 0 & 0 \\ 0 & 0 & 0 & 0 & 0 & 0 & 0 & 0 & 0 & 0 & 0 & 0 & 0 \\ 0 & 0 & 0 & 0 & 0 & 0 & 0 & 0 & 0 & 0 & 0 & 0 & 0 \\ 0 & 0 & 0 & 0 & 0 & 0 & 0 & 0 & 0 & 0 & 0 & 0 & 0 \\ 0 & 0 & 0 & 0 & 0 & 0 & 0 & 0 & 0 & 0 & 0 & 0 & 0 \\ 0 & 0 & 0 & 0 & 0 & 0 & 0 & 0 & 0 & 0 & 0 & 0 & 0 \\ 0 & 0 & 0 & 0 & 0 & 0 & 0 & 0 & 0 & 0 & 0 & 0 & 0 \\ 0 & 0 & 0 & 0 & 0 & 0 & 0 & 0 & 0 & 0 & 0 & 0 & 0 \end{bmatrix} \quad 3.14$$

Where,

$$a_{41} = \frac{1}{(C_m + R_m)(C_a + R_{a1} + C_c + R_{c1})} - \frac{1}{R_{c2}(C_c + R_{c1})}$$

$$a_{44} = -\frac{1}{R_{c2}(C_c + R_{c1})} \qquad a_{45} = \frac{E_m}{(C_m + R_m)(C_a + R_{a1} + C_c + R_{c1})}$$

$$a_{46} = \frac{E_m}{C_m + R_m} - I \qquad a_{47} = \frac{E_a}{R_{a2}(C_a + R_{a1})}$$

$$a_{48} = \frac{E_a}{C_a + R_{a1}} \qquad a_{49} = \frac{E_a}{R_{c2}} - I$$

$$a_{4,10} = \frac{E_c}{R_{c2}(C_c + R_{c1})} \qquad a_{4,11} = \frac{E_c}{C_c + R_{c1}}$$

$$a_{4,12} = \frac{E_c}{R_{c2}} - I$$

$$a_{4,13} = -\frac{1}{R_{c2}(C_c + R_{c1})}\left[E_{cell} + E_m + E_a + (X_L + R_0) - E_{cell(orp)}\right] - I$$

And the measurement matrix, H as:

$$H = [0 \quad 0 \quad 0 \quad 1 \quad 0 \quad 0 \quad 0 \quad 0 \quad 0 \quad 0 \quad 0 \quad 0 \quad 0] \qquad 3.15$$

EKF of approximate circuit for V-RFB

Form of (3.9) is used to illustrate state variable of the parameter of actual circuit for V-RFB by applying equations (3.7) and (3.8) for model development. State x_k as:

$$x_k = [E_p \quad E_{cell} \quad Z_a \quad Z_c \quad Z_m \quad Z_L]^T \qquad 3.16$$

From state model with deliberation of input variable:

$$f(x_k, u_k) = [f_1 \quad f_2 \quad f_3 \quad f_4 \quad f_5 \quad f_6\,]^T \qquad 33.17$$

$$z_k = h_k(x_k) = [0 \quad E_{cellk} \quad 0 \quad 0 \quad 0 \quad 0]^T \qquad 33.18$$

Where $u_k = I$, f is the transition matrix of V-RFB system, and h_k is measurement matrix. Thus, $f_s(s = 1, 2, 3, 4, 5, 6)$ are describe as:

From (3.7), $f_1 = -x_1/((x_3 + x_4) * x_5) + u_k/x_5$

From (3.8), $f_2 = -x_2 + x_1/((x_3 + x_4) - (x_6 * u_k) - u_k/x_5 + E_{cell(orp)}$

Thus, $f_3 = f_4 = f_5 = f_6 = 0$ 3.19

From (3.18) the matrix representation of the model, F is calculated as:

$$F = \frac{\partial f}{\partial x}|x = \hat{x} = \begin{bmatrix} a_{11} & 0 & a_{13} & a_{14} & a_{15} & 0 \\ a_{21} & 0 & a_{23} & a_{24} & a_{25} & a_{26} \\ 0 & 0 & 0 & 0 & 0 & 0 \\ 0 & 0 & 0 & 0 & 0 & 0 \\ 0 & 0 & 0 & 0 & 0 & 0 \\ 0 & 0 & 0 & 0 & 0 & 0 \end{bmatrix} \qquad 3.20$$

Where,

$$a_{11} = -\frac{1}{(Z_a + Z_c)Z_m} \qquad a_{13} = -\frac{E_p}{Z_m(Z_a + Z_c)}$$

$$a_{14} = -\frac{E_p}{Z_a + Z_c} \qquad a_{15} = -\frac{E_p}{Z_m} - I$$

$$a_{21} = \frac{1}{(Z_a + Z_c)Z_m} \qquad a_{23} = \frac{E_p}{Z_a + Z_c}$$

$$a_{24} = \frac{E_p}{Z_a + Z_c} \qquad a_{25} = \frac{Ep}{Z_m} - I$$

$$a_{26} = -\left[E_{cell} + E_p + \left(\frac{1}{Z_m} + Z_L\right) - E_{cell(orp)}\right] - I$$

And the measurement matrix, H as:

$$H = [\,0 \quad 0 \quad 1 \quad 0 \quad 0 \quad 0\,] \qquad 3.21$$

3.5 Simulation and result analyzation

MATLAB software was used to simulate the circuits using EKF method. EKF algorithms were formed based on the derivation from both actual and approximate circuits. Simulation for both circuits was conducted respectively to estimate the parameters. Tuning process was involved as the graphs obtained from the simulations diverged. This process needed to be carried out constantly until the graph of each parameter of both circuits approaches a steady state. The graph simulation for the circuits is analysed accordingly.

3.6 Chapter conclusion

This chapter begins with the discussion of the flow of the project; from the derivation of the equivalent circuits for V-RFB to the analyses of the results. Both actual and approximate circuit for V-RFB were derived accordingly. From the derivation of the circuits, EKF was used as parameter estimation to simulate both circuits. The graph of each parameter of actual and approximate circuit was observed and analysed. Tuning processes continuously took place until a steady state graph of each parameter for both circuits was obtained. As the parameter in each graph approaches a steady state, it shows the compatibility of the circuit itself. The processes then continued until the objectives of the project were achieved.

CHAPTER 4

RESULTS AND DISCUSSIONS

4.1 Chapter overview

This chapter focuses on the results of both actual and approximate circuit for V-RFB. The result shows the graph for each parameter of circuits is in a steady state. All data were capture at 80% SOC. Result of an error is also shown to see the efficiency of the equivalent circuit for V-RFB.

4.2 Open Circuit Voltage

OCV or $E_{cell(orp)}$ refers to as State of Charge (SOC) function and directly related. To validate the model, verification of the OCV curve is one of the options. The accuracy of OCV estimation influences the battery SOC accuracy. Simulation was conducted for both circuits and tuning process was also taken place in order to gain a steady state graph of each parameter of both circuits. All data were capture at 80% of SOC. Figure 4.1 shows a comparison between EKF-based estimated and experimental E_{cell} of equivalent electrical circuit that charged at 1.5 V and discharged at minimum 1.46 V. Meanwhile, Figure 4.2 shows a comparison between EKF-based estimated and experimental E_{cell} of approximate circuit which was also charged at 1.5 V while discharged at minimum 1.35 V. It can be observed that for equivalent electrical circuit that $E_{cell\ EKF\ estimation}$ and $E_{cell\ experiment}$ are overlapped with minor within 50s, whereas for approximate circuit that $E_{cell\ EKF\ estimation}$ and $E_{cell\ experiment}$ are overlapped with minor differences within 100s. Based on this observation it is proven that both circuits are suitable for V-RFB, even though there is inconsistency at the first 50s. This inconsistency occur due to high measurement noise covariance, however both circuit achieved steady state within 50s and 100s respectively. Constant current (1.5A) is applied for both circuit due to the parasitic inductance which can affect the immediate voltage drop of cell voltage during discharge and could cause under voltage if high current density is used. It takes some times for the cell voltage of experiment and EKF estimation to stabilize as the inductor oppose changes.

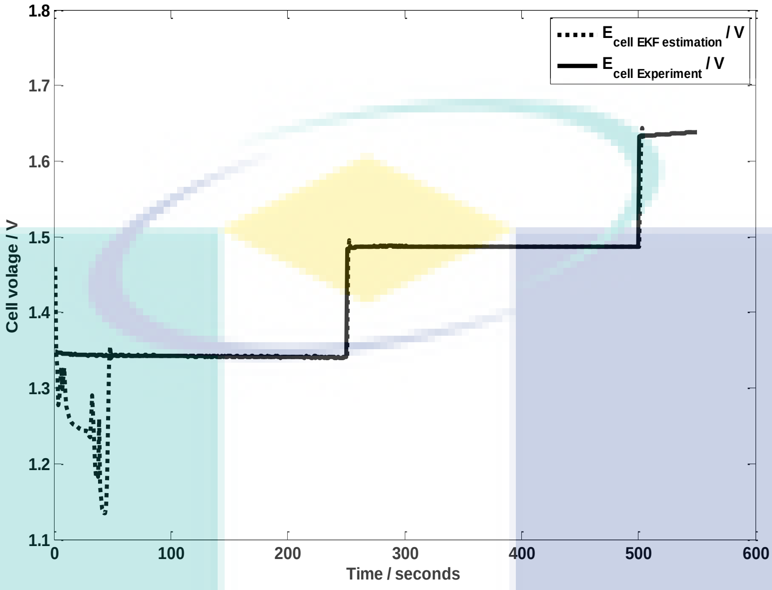

Figure 4.1 Comparison of EKF-based estimated and experimental E_{cell} of equivalent electrical circuit at 80% of SOC.

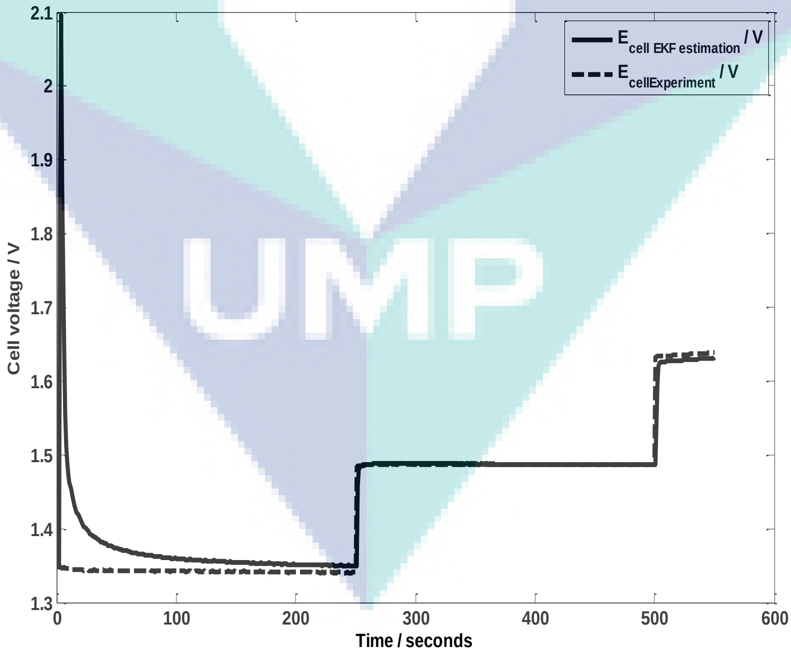

Figure 4.2 Comparison of EKF-based estimated and experimental E_{cell} of approximate circuit at 80% of SOC

The accuracy state vector estimation performance is illustrated in Figure 4.3 and Figure 4.4. Figure 4.3 shows the degree of uncertainties of state estimation covariance for actual circuit, and as observed all state estimation approach a steady state at the end. Figure 4.4 shows the degree of uncertainties of state estimation covariance for the approximate circuit, and in the end all state estimations approach steady states. Both circuit states estimation shows approaching steady state so it depicts the performance and accuracy of the estimated state.

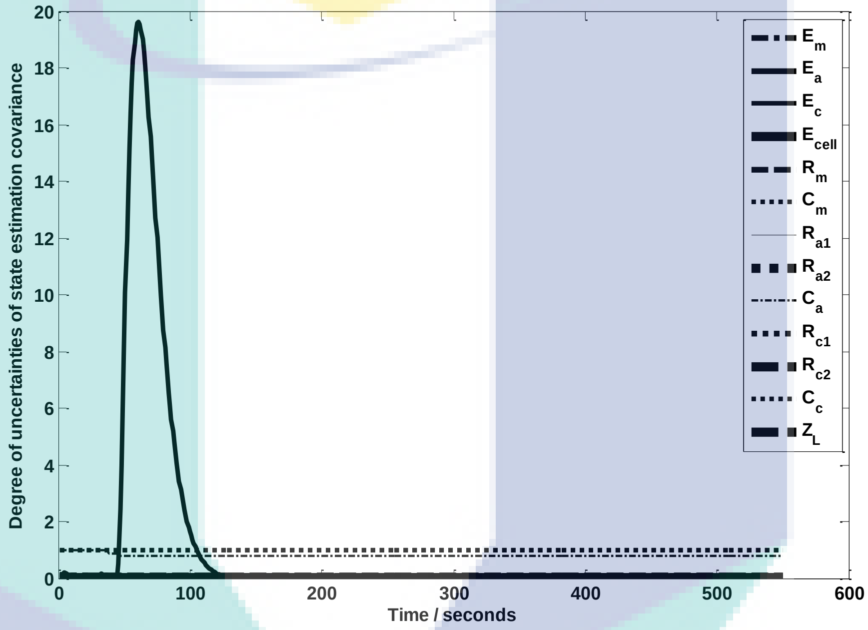

Figure 4.3 Degree of uncertainties of state estimation covariance for equivalent electrical circuit at 80% of SOC.

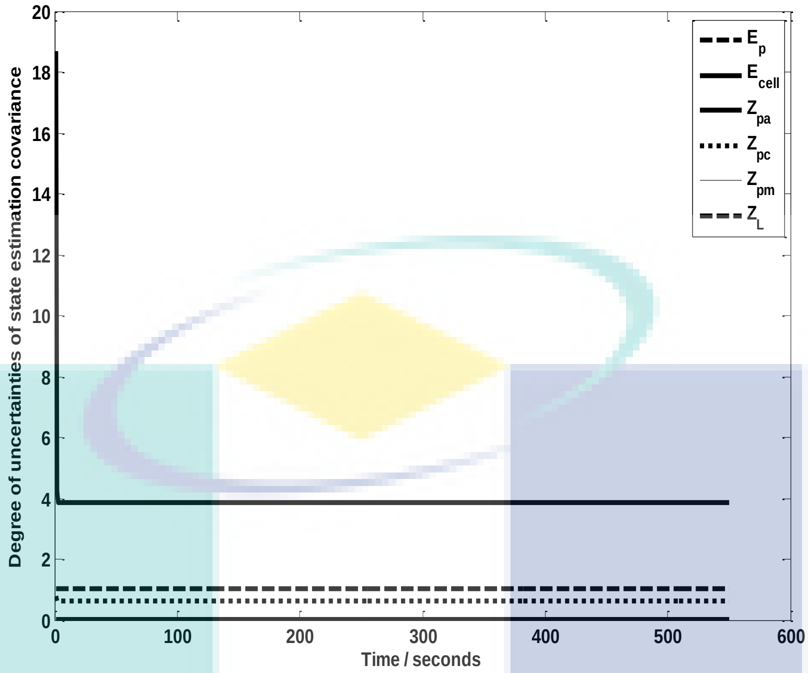

Figure 4.4 Degree of uncertainties of state estimation covariance for approximate circuit at 80% of SOC.

4.3 Polarization

Polarization is also known as losses which usually occurs at activation, concentration, and ohmic polarization (Yu & Yuvarajan, 2005). Current density influences the losses to occur, as a high current transient is applied, parasitic elements can affect the systems performance. As for activation polarization, the losses increase as the current increases and shows the slowest step in electrochemical reaction. Concentration polarization occurs at only high current and can be reduced as the formation large positive ions at electrode/electrolyte interface. Resistor is referred as the losses of ohmic from the electrodes and electrolyte electrical resistance. Ohmic resistance loss and the relaxation period voltage drop related before the transient mode start although the capacitance and the battery transient behaviour can be related. Mass transfer is essential in controlling the success and rate any preparative electrochemical reaction easily measureable and predictable. Subtopic 4. 3. 1 and 4. 3. 2 shows the results of activation, concentration, and mass transport polarization of both actual and approximate circuit.

4.3.1 Equivalent electrical circuit

The estimation of parameters of the V-RFB based on the implemented EKF model against time and all the data recorded at discharging mode at 80% of SOC are illustrated as capacitance mass transfer (C_m), resistance mass transfer(R_m), capacitance activation polarization (C_a), resistance activation polarization $(R_{a1}\ and\ R_{a2})$, capacitance concentration polarization (C_c), resistance concentration polarization $(R_{c1}\ and\ R_{c2})$, parasitic inductance (X_L) and estimation error$(E_{cell}\ error)$ respectively in Figure 4.5 until Figure 4.14. Tuning process of the simulation continuously takes place until the graph of each parameter approaches a steady state.

The tuning of covariance of P (initial state), Q (process noise), and R (measurement noise) are expressed as follows:

$$P = \begin{bmatrix} 4e^{-2} & 0 & 0 & 0 & 0 & 0 & 0 & 0 & 0 & 0 & 0 & 0 & 0 \\ 0 & 5e^{-8} & 0 & 0 & 0 & 0 & 0 & 0 & 0 & 0 & 0 & 0 & 0 \\ 0 & 0 & 8e^{-2} & 0 & 0 & 0 & 0 & 0 & 0 & 0 & 0 & 0 & 0 \\ 0 & 0 & 0 & 1e^{-2} & 0 & 0 & 0 & 0 & 0 & 0 & 0 & 0 & 0 \\ 0 & 0 & 0 & 0 & 1e^{-1} & 0 & 0 & 0 & 0 & 0 & 0 & 0 & 0 \\ 0 & 0 & 0 & 0 & 0 & 1 & 0 & 0 & 0 & 0 & 0 & 0 & 0 \\ 0 & 0 & 0 & 0 & 0 & 0 & 1e^{-1} & 0 & 0 & 0 & 0 & 0 & 0 \\ 0 & 0 & 0 & 0 & 0 & 0 & 0 & 1e^{-1} & 0 & 0 & 0 & 0 & 0 \\ 0 & 0 & 0 & 0 & 0 & 0 & 0 & 0 & 1 & 0 & 0 & 0 & 0 \\ 0 & 0 & 0 & 0 & 0 & 0 & 0 & 0 & 0 & 1e^{-1} & 0 & 0 & 0 \\ 0 & 0 & 0 & 0 & 0 & 0 & 0 & 0 & 0 & 0 & 1e^{-1} & 0 & 0 \\ 0 & 0 & 0 & 0 & 0 & 0 & 0 & 0 & 0 & 0 & 0 & 1 & 0 \\ 0 & 0 & 0 & 0 & 0 & 0 & 0 & 0 & 0 & 0 & 0 & 0 & 1 \end{bmatrix}$$

$$Q = \begin{bmatrix} 1e^{-4} & 0 & 0 & 0 & 0 & 0 & 0 & 0 & 0 & 0 & 0 & 0 & 0 \\ 0 & 1e^{-4} & 0 & 0 & 0 & 0 & 0 & 0 & 0 & 0 & 0 & 0 & 0 \\ 0 & 0 & 1e^{-4} & 0 & 0 & 0 & 0 & 0 & 0 & 0 & 0 & 0 & 0 \\ 0 & 0 & 0 & 1e^{-4} & 0 & 0 & 0 & 0 & 0 & 0 & 0 & 0 & 0 \\ 0 & 0 & 0 & 0 & 0 & 0 & 0 & 0 & 0 & 0 & 0 & 0 & 0 \\ 0 & 0 & 0 & 0 & 0 & 0 & 0 & 0 & 0 & 0 & 0 & 0 & 0 \\ 0 & 0 & 0 & 0 & 0 & 0 & 0 & 0 & 0 & 0 & 0 & 0 & 0 \\ 0 & 0 & 0 & 0 & 0 & 0 & 0 & 0 & 0 & 0 & 0 & 0 & 0 \\ 0 & 0 & 0 & 0 & 0 & 0 & 0 & 0 & 0 & 0 & 0 & 0 & 0 \\ 0 & 0 & 0 & 0 & 0 & 0 & 0 & 0 & 0 & 0 & 0 & 0 & 0 \\ 0 & 0 & 0 & 0 & 0 & 0 & 0 & 0 & 0 & 0 & 0 & 0 & 0 \\ 0 & 0 & 0 & 0 & 0 & 0 & 0 & 0 & 0 & 0 & 0 & 0 & 0 \\ 0 & 0 & 0 & 0 & 0 & 0 & 0 & 0 & 0 & 0 & 0 & 0 & 0 \end{bmatrix}$$

$$R = [1e^{-5}]$$

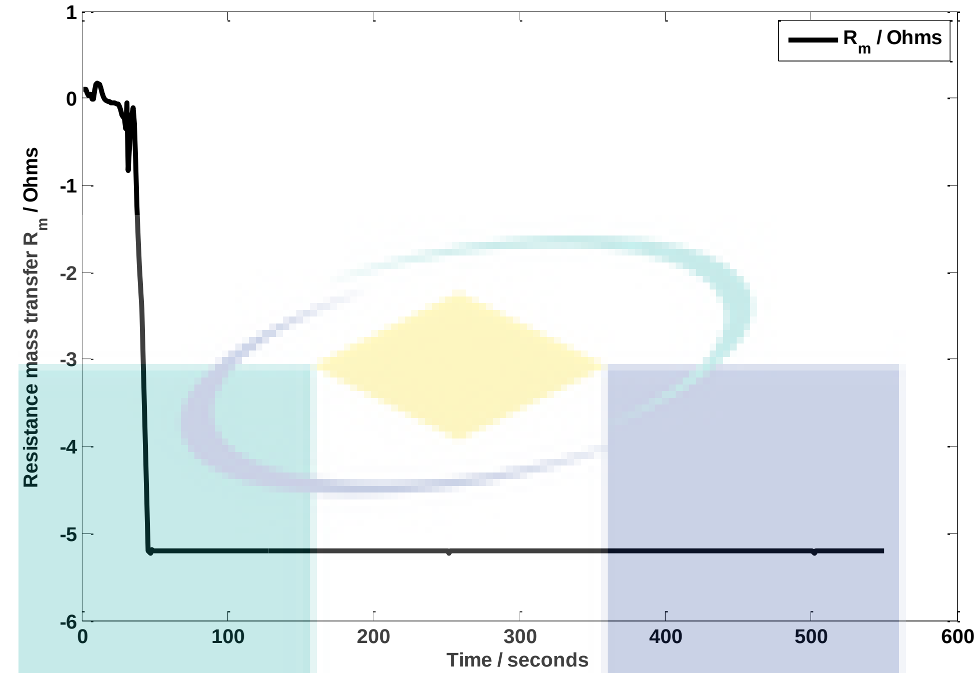

Figure 4.5 Estimation result of resistance mass transfer polarization of equivalent electrical circuit for V-RFB

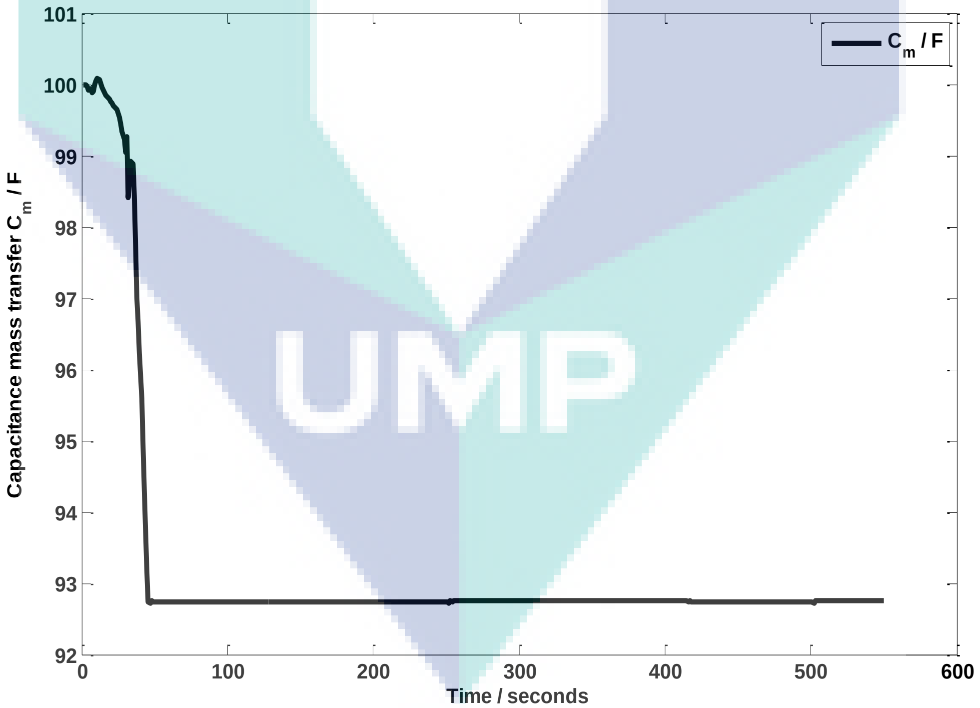

Figure 4.6 Estimation result of capacitance mass transfer polarization of equivalent electrical circuit for V-RFB

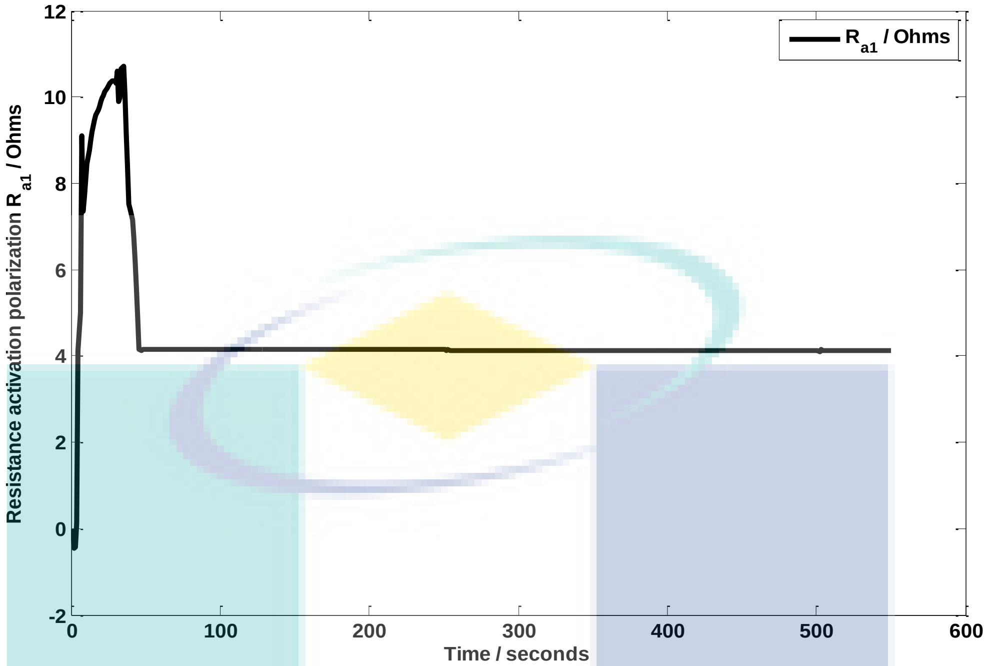

Figure 4.7 Estimation result of resistance activation polarization (1) of equivalent electrical circuit for V-RFB

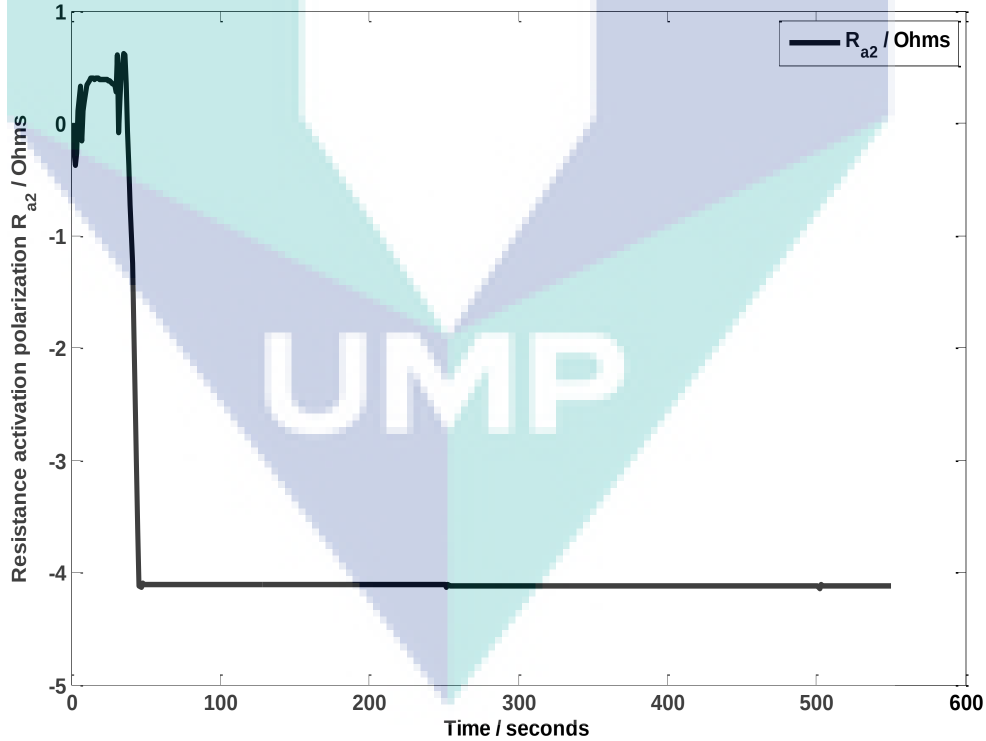

Figure 4.8 Estimation result of resistance activation polarization (2) of equivalent electrical circuit for V-RFB

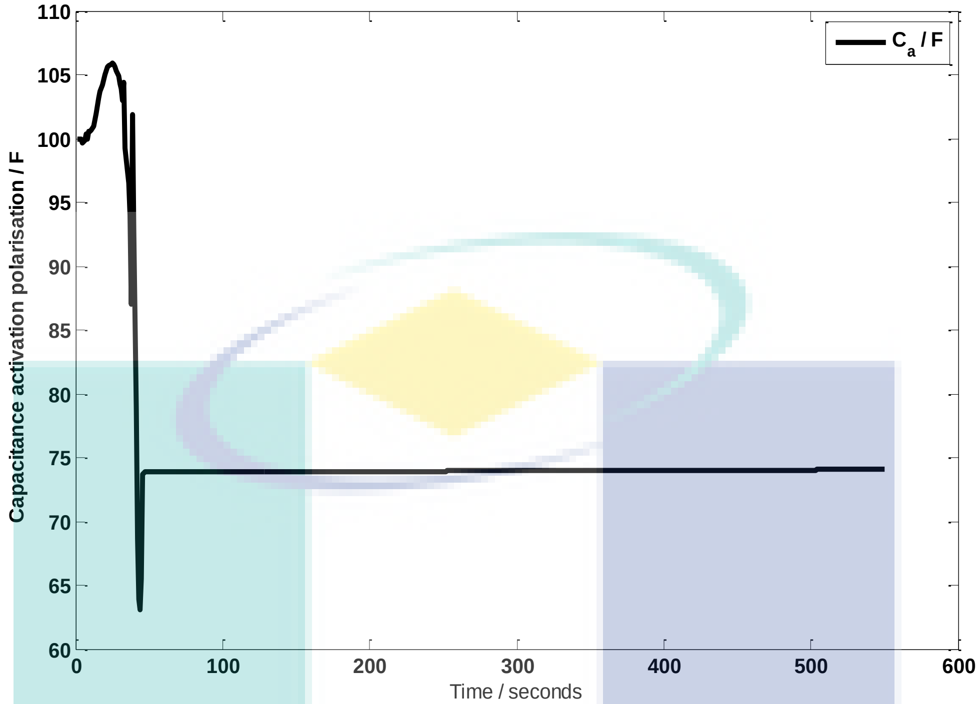

Figure 4.9 Estimation result of capacitance activation polarization of equivalent electrical circuit for V-RFB

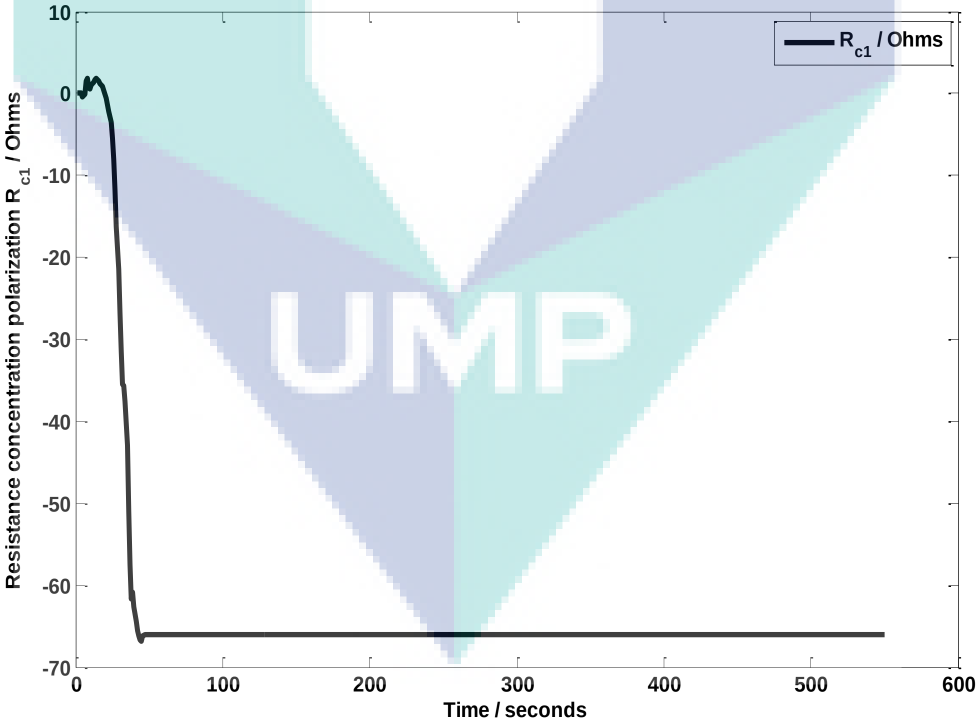

Figure 4.10 Estimation result of resistance concentration polarization (1) of equivalent electrical circuit for V-RFB

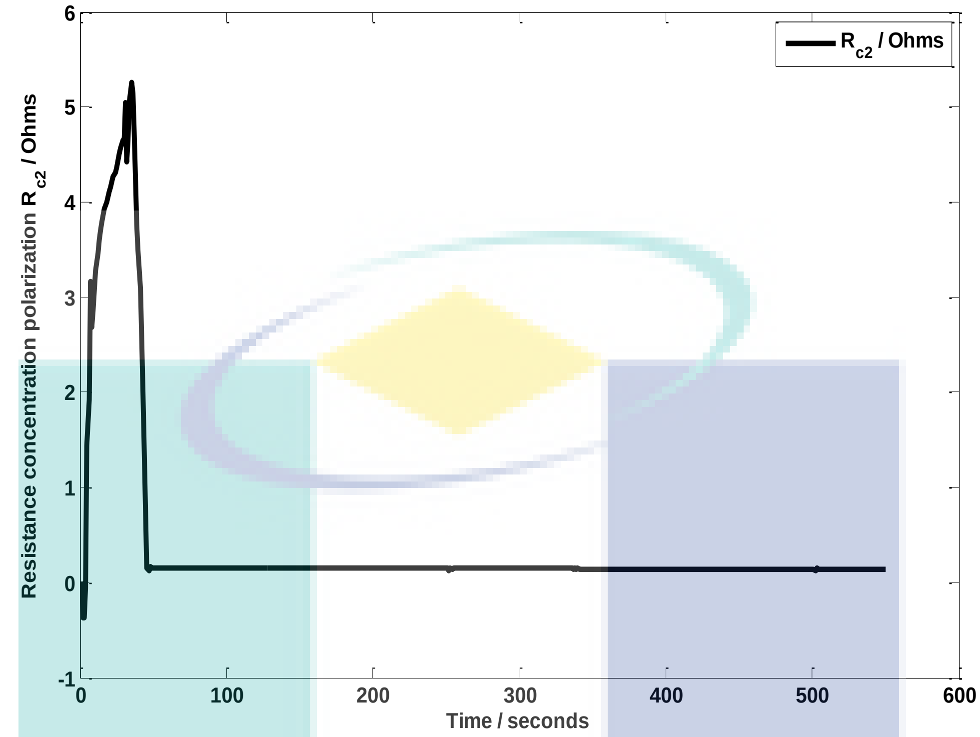

Figure 4.11 Estimation result of resistance concentration polarization (2) of equivalent electrical circuit for V-RFB

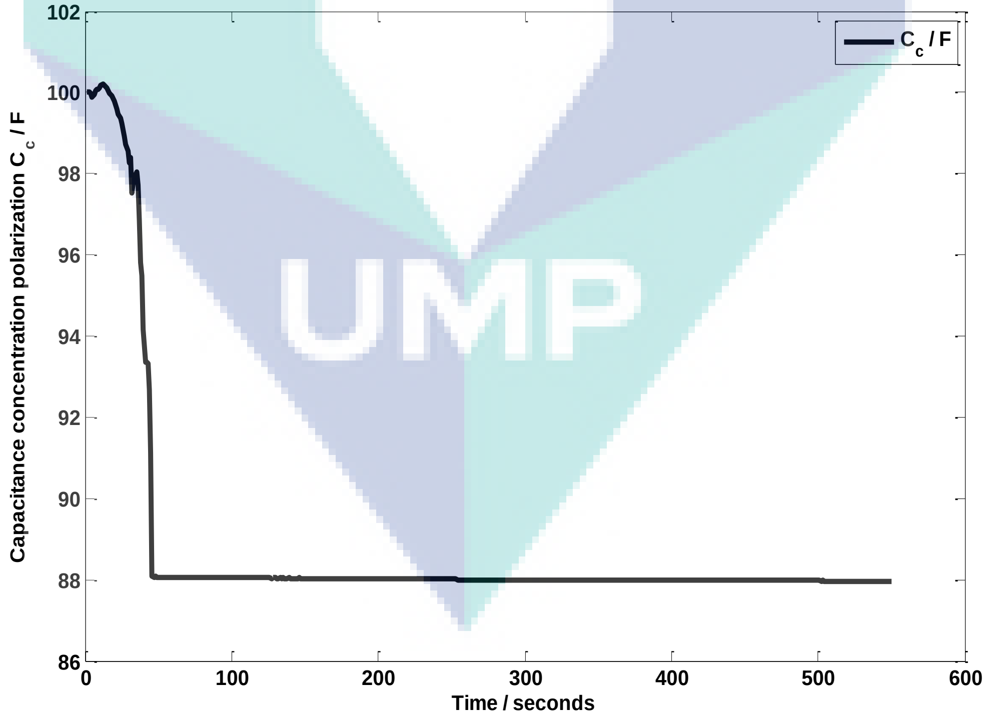

Figure 4.12 Estimation result of capacitance concentration polarization of equivalent electrical circuit for V-RFB

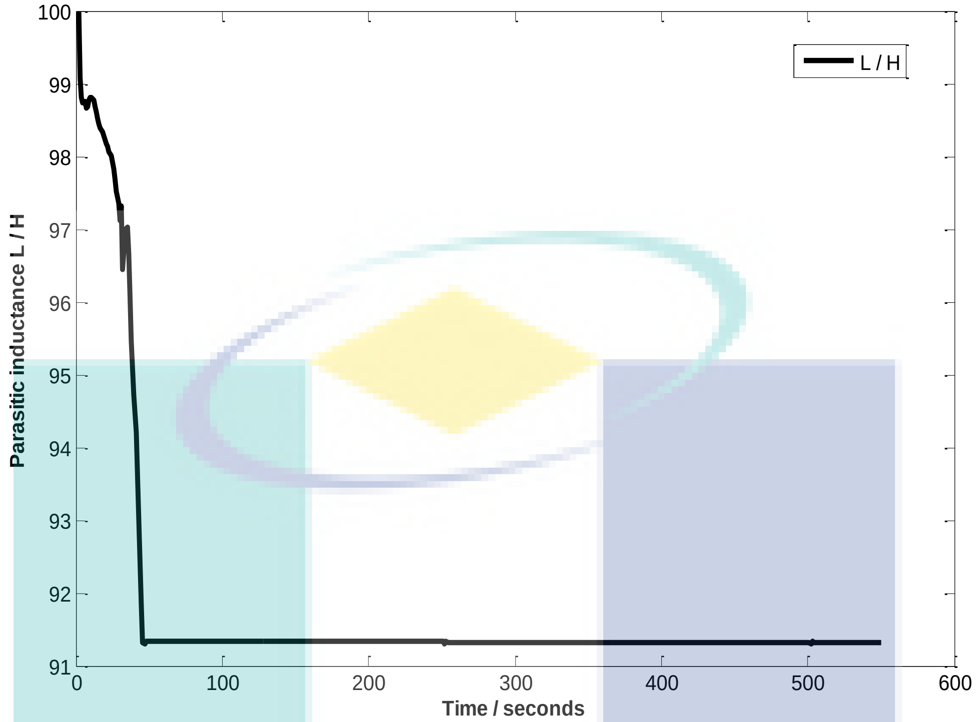

Figure 4.13 Estimation result of parasitic inductance of equivalent electrical circuit for V-RFB

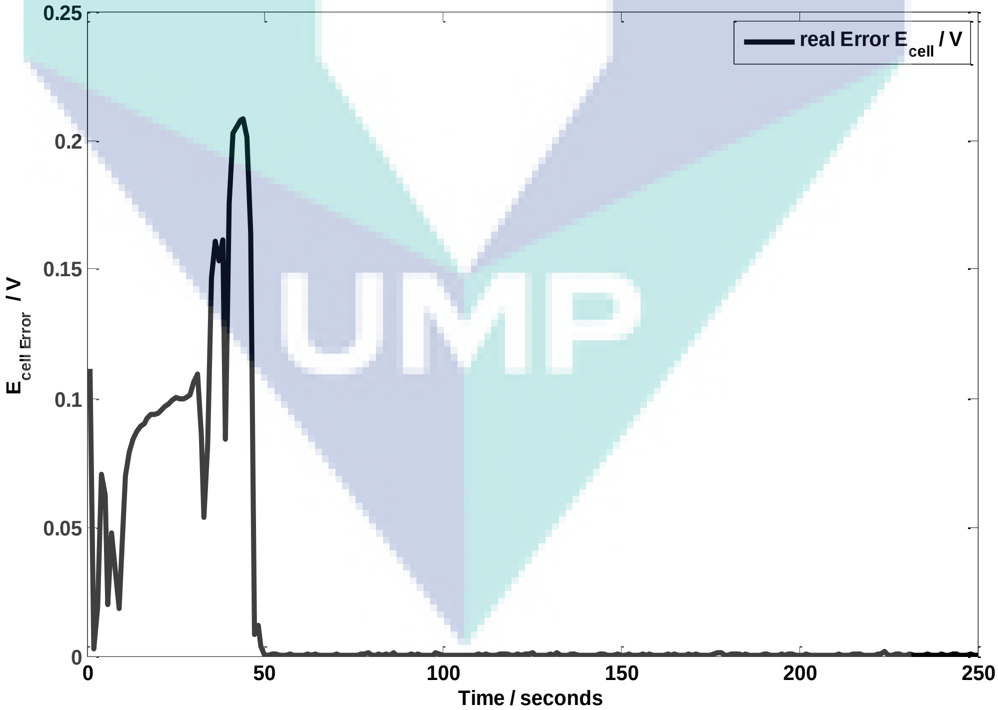

Figure 4.14 Estimation result of E_{cell} error of equivalent electrical circuit for V-RFB

The mass transfer, activation and concentration polarization of resistance and capacitance along with parasitic inductance illustrated in Figure 4.5 until Figure 4.13 at 80% SOC, as observed within the first 40s at each estimated parameters prior to approaching a steady state. Hence, the stability of the circuit by implementing EKF as a parameter estimation is evident as the graph for each parameter approaches a steady state. The small value of error indicates the accuracy of the system's result; as shown in Figure 4.14 the error for equivalent electrical circuit is 0.6%.

4.3.2 Approximate circuit

The estimation of parameters of the V-RFB based on the implemented EKF model against time and all the data recorded at discharging mode at 80% of SOC are illustrated as impedance of activation polarization (Z_a), concentration polarisation (Z_c), mass transfer (Z_m) and parasitic inductance (Z_L), and also estimation error $(E_{cell}\ error)$ respectively in Figure 4.15 until Figure 4.19.

The tuning of covariance of P (initial state), Q (process noise), and R (measurement noise) are expressed as follows:

$$P = \begin{bmatrix} 6e^{-2} & 0 & 0 & 0 & 0 & 0 \\ 0 & 1e^{-2} & 0 & 0 & 0 & 0 \\ 0 & 0 & 1 & 0 & 0 & 0 \\ 0 & 0 & 0 & 6e^{-1} & 0 & 0 \\ 0 & 0 & 0 & 0 & 7e^{-6} & 0 \\ 0 & 0 & 0 & 0 & 0 & 1 \end{bmatrix}$$

$$Q = \begin{bmatrix} 1e^{-4} & 0 & 0 & 0 & 0 & 0 \\ 0 & 1e^{-4} & 0 & 0 & 0 & 0 \\ 0 & 0 & 1e^{-4} & 0 & 0 & 0 \\ 0 & 0 & 0 & 0 & 0 & 0 \\ 0 & 0 & 0 & 0 & 0 & 0 \\ 0 & 0 & 0 & 0 & 0 & 0 \end{bmatrix}$$

$$R = 1e^{-5}$$

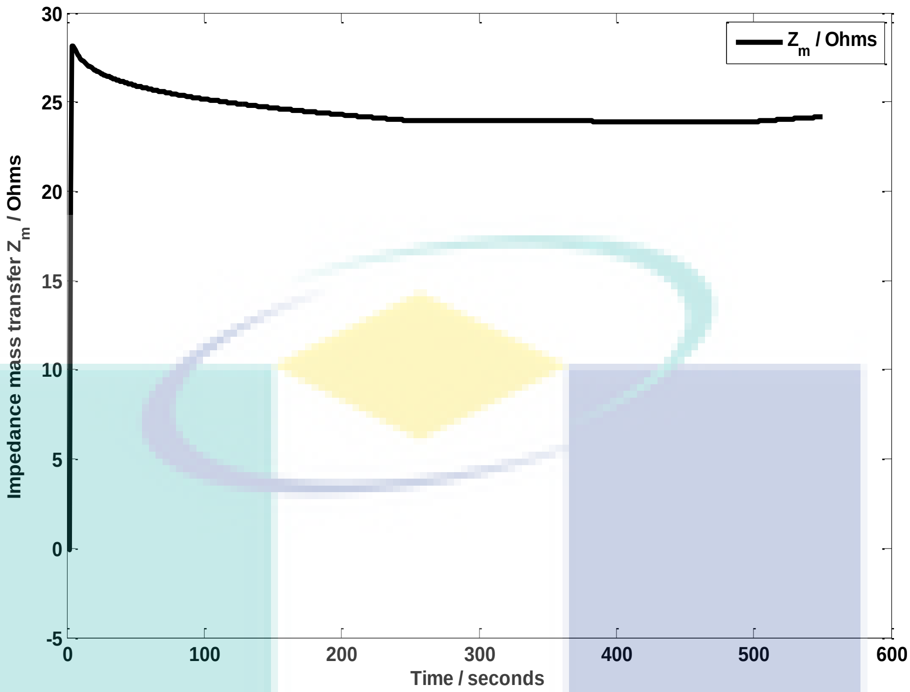

Figure 4.15 Estimation result of impedance mass transfer of approximate circuit for V-RFB

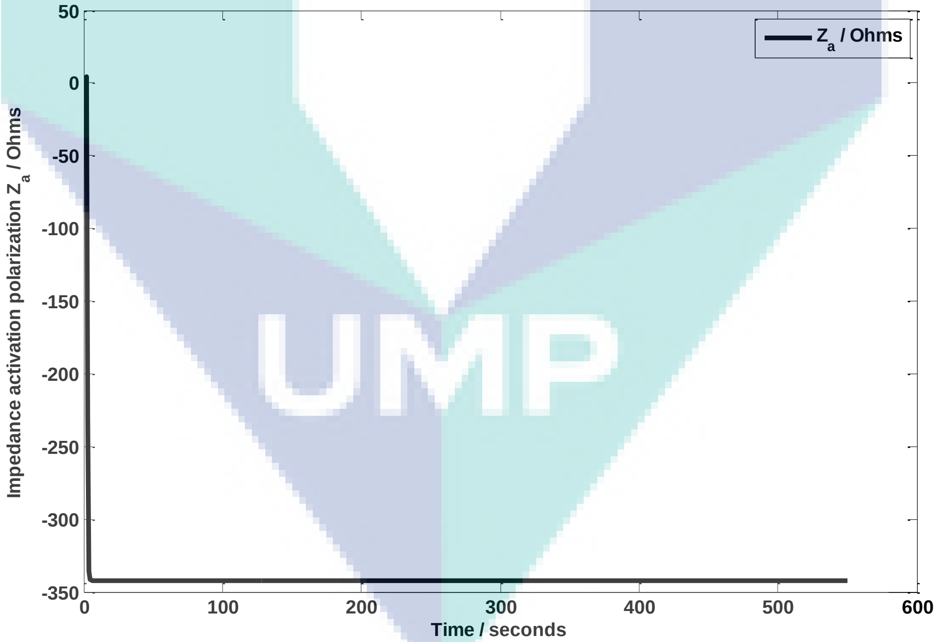

Figure 4.16 Estimation result of impedance activation polarization of approximate circuit for V-RFB

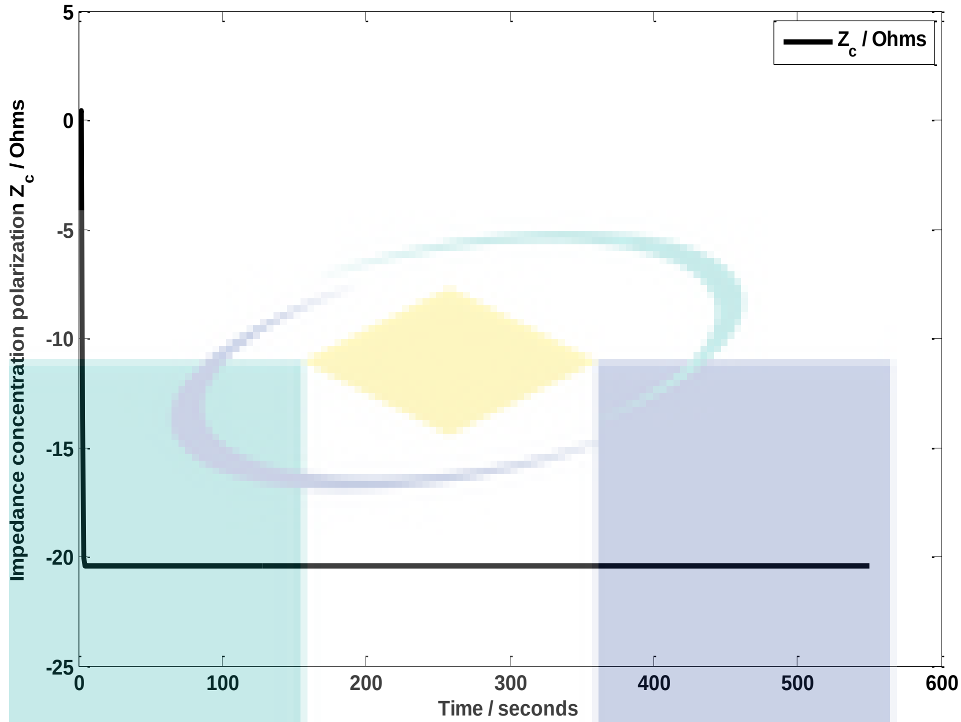

Figure 4.17 Estimation result of impedance concentration of approximate circuit for V-RFB

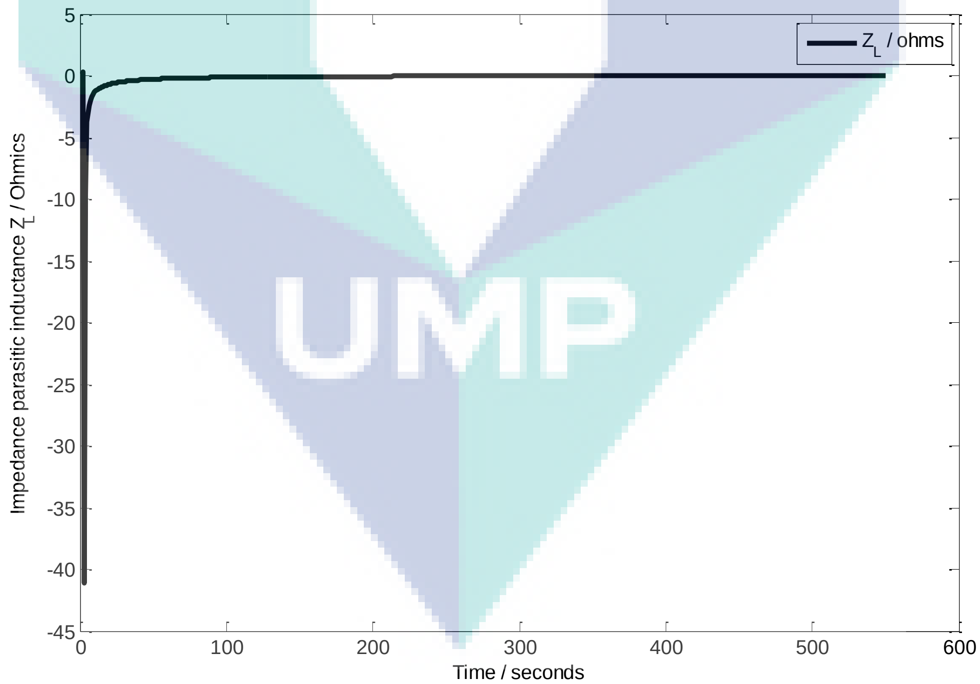

Figure 4.18 Estimation result of impedance parasitic inductanceof approximate circuit for V-RFB

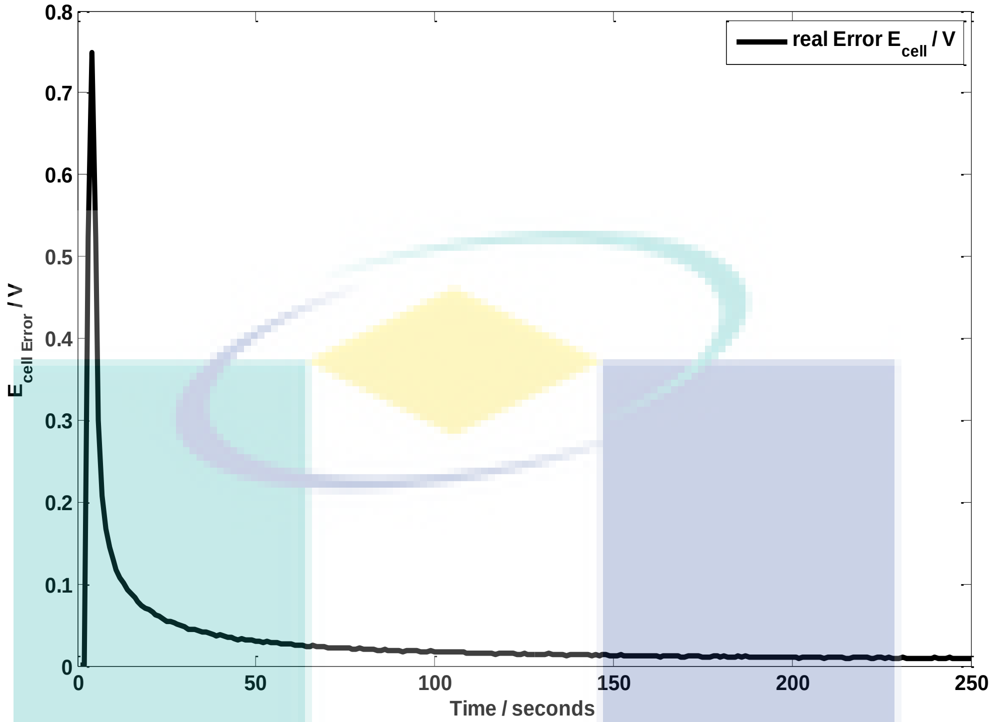

Figure 4.19 Estimation result of cell voltage error of approximate circuit for V-RFB

The impedance of mass transfer, activation and concentration polarization and also parasitic inductance are illustrated in Figure 4.15 until Figure 4.19 at 80% SOC, as observed within less than 10s the estimated parameter reached a steady state within the first few seconds. The small value of error indicates the accuracy of the system's result, as shown in Figure 4.19 in which the error for the approximate circuit is 2.0%.

It is vital to be consistent when evaluating the filter performance because the estimation vector can be affected. Based on both actual and approximate circuits, for each parameter of the circuit, the behaviour of the estimation approaches a steady state with 0.6% and 2.0% errors, respectively. As the error shows closer to zero it can be proven that both circuits are adaptable in any V-RFB systems. Both circuits approach a steady state at less than 10s and 40s, respectively, as reported in the previous work (M. R. Mohamed et al., 2013) that the proposed circuit achieved a steady state after 150s. This demonstrated that the circuit in this project is compatible for V-RFB.

4.4 Chapter conclusion

In this chapter, the result for each parameter of actual and approximate circuit for V-RFB shows that the state estimation smoothly approaches a steady state at the end with 0.6% and 2.0% errors, respectively. Hence, it proves the stability of the circuits as the error is closer to zero. As shown in Figure 4.1 and 4.2, both circuits shows adaptability to represent V-RFB as estimation EKF-based and experiment cell voltage are overlapped with minor differences. Furthermore, the estimation result of all states for actual and approximate circuit shows approaching steady state. Based on the result, EKF is proven as the suitable method for parameter estimation due to both circuit shows the adaptiveness for V-RFB. So, it is also depicts that the approximate circuit can be an alternative of actual circuit for V-RFB.

CHAPTER 5

CONCLUSION & RECOMMENDATION

5.1 Conclusion

Vanadium Redox Flow Battery is promising as an energy storage technology and in the future it would be widely used. Based on the research, equivalent circuit for V-RFB is presented, which can be categorised into actual and approximate circuit. Both circuit was derived accordingly and then estimated using EKF algorithm. Approximate circuit is formed as an alternative for actual circuit by lumped some of the parameters. This is to reduce the complexity in represent the simulation result and also time.

The result of parameter estimation by using EKF method of estimated EKF-based and experiment cell voltage for both circuit are overlapped and estimation of each parameter for both circuits shows approaching steady state. Therefore, it is proven that actual and approximate circuit are adaptable for V-RFB and also approximate circuit as an alternative for actual circuit. The effectiveness of the model simulation verifies where the error is closer to zero; 0.6% and 2.0% errors, respectively. Thus, it is also proven that EKF mothed is one of the best choices for parameter estimation.

5.2 Recommendation

Based on the presented result of parameters high value of noises can affect the estimation of the system. Continuous research on the equivalent circuit for Vanadium Redox Flow Battery (V-RFB) can be take place by authenticate using Kalman Filter at different SOC and circuit to validate the system. It is recommended that further research is undertaken in the following areas: size of channel, pore diameter, and effect of an applied catalyst on graphite felt. All these areas of research would be a great help to fully study the behaviour of V-RFB system. Further investigation on the thermal response on different V-RFB cell designs is strongly recommended.

REFERENCES

Arenas, L. F., León, C. P. De, & Walsh, F. C. (2017). Engineering aspects of the design, construction

and performance of modular redox fl ow batteries for energy storage. Journal of Energy Storage,

11, 119–153. https://doi.org/10.1016/j.est.2017.02.007.

Arnold, C. B. (2011). Batteries and Energy Storage. Journal of The Electrochemical …. Retrieved from http://jes.ecsdl.org/content/159/1/A26.short.

Alotto, P., Guarnieri, M., & Moro, F. (2013). Redox flow batteries for the storage of renewable energy: A review. Renewable and Sustainable Energy Reviews, 29, 325–335. http://doi.org/10.1016/j.rser.2013.08.001.

Alotto, P., Guarnieri, M., Moro, F., & Stella, A. (2012). Redox Flow Batteries for large scale energy storage. 2012 IEEE International Energy Conference and Exhibition, ENERGYCON 2012, 293–298. https://doi.org/10.1109/EnergyCon.2012.6347770.

Aaron, D. S., Liu, Q., Tang, Z., Grim, G. M., Papandrew, A. B., Turhan, A., … Mench, M. M. (2012). Dramatic performance gains in vanadium redox flow batteries through modified cell architecture. Journal of Power Sources, 206, 450–453. https://doi.org/10.1016/j.jpowsour.2011.12.026.

Bhattarai, A., Wai, N., Schweiss, R., Whitehead, A., Lim, T. M., & Hng, H. H. (2017). Advanced porous electrodes with flow channels for vanadium redox flow battery. Journal of Power Sources, 341, 83–90. https://doi.org/10.1016/j.jpowsour.2016.11.113.

Byrne, R., & Macartain, P. (1999). Energy Performance of an Operating 50 kWh Zinc-Bromide Flow Battery System. 2015 IEEE International Conference on Engineering, Technology and Innovation/ International Technology Management Conference (ICE/ITMC), 13(6), 142–148. https://doi.org/10.1109/ICE.2015.7438688.

Banani, S. a. (2007). A New Version of Unscented Kalman Filter, 1(2), 1–6.

Blanc, C., Member, S., & Rufer, I. A. (2008). Multiphysics and Energetic Modeling of a Vanadium Redox Flow Battery. IEEE, International Conference on Sustainable Energy Storage Technologies.

Bortolin, S., Toninelli, P., Maggiolo, D., Guarnieri, M., & Del Col, D. (2015). CFD study on electrolyte distribution in redox flow batteries. Journal of Physics: Conference Series, 655(November), 12049. https://doi.org/10.1088/1742-6596/655/1/012049.

Blanc, C. (2016). Modeling of a vanadium redox flow battery electricity storage system, (April). http://doi.org/10.5075/epfl-thesis-4277.

Blanc, C., & Rufer, A. (2010). Understanding the Vanadium Redox Flow Batteries. Paths to Sustainable Energy, (July 2016), 333–358. http://doi.org/10.5772/13338.

Brown, L. D., Neville, T. P., Jervis, R., Mason, T. J., Shearing, P. R., & Brett, D. J. L. (2016). The effect of felt compression on the performance and pressure drop of all-vanadium redox flow batteries. Journal of Energy Storage, 8, 91–98. https://doi.org/10.1016/j.est.2016.10.003.

Chakrabarti, M. H., Brandon, N. P., Hajimolana, S. A., Tariq, F., Yufit, V., Hashim, M. A., Aravind, P. V. (2014). Application of carbon materials in redox flow batteries. Journal of Power Sources, 253, 150–166. https://doi.org/10.1016/j.jpowsour.2013.12.038.

Choi, W., Enjeti, P. N., & Howze, J. W. (2004). Development of an equivalent circuit model of a fuel cell to evaluate the effects of inverter ripple current. Paper presented at the Nineteenth Annual IEEE Applied Power Electronics Conference and Exposition, 2004. APEC'04.

Chahwan, J., Abbey, C., & Joos, G. (2007). VRB modelling for the study of output terminal voltages, internal losses and performance. 2007 IEEE Canada Electrical Power Conference, EPC 2007, 387–392. http://doi.org/10.1109/EPC.2007.4520363.

Chang, W.-Y. (2013). Estimating equivalent circuit parameters of proton exchange membrane fuel cell using the current change method. International Journal of Electrical Power & Energy Systems, 53, 584–591. http://doi.org/10.1016/j.ijepes.2013.05.031.

Chen, H., Cong, T. N., Yang, W., Tan, C., Li, Y., & Ding, Y. (2009). Progress in electrical energy storage system: A critical review. Progress in Natural Science, 19(3), 291–312. http://doi.org/10.1016/j.pnsc.2008.07.014.

Cervantes-Alcala, R., & Miranda-Hernandez, M. (2018). Flow distribution and mass transport analysis in cell geometries for redox flow batteries through computational fluid dynamics. Journal of Applied Electrochemistry, online ver(0), 1–12. https://doi.org/10.1007/s10800-018-1246-7.

Chen, D., Hickner, M. A., Agar, E., & Kumbur, E. C. (2013). Optimizing membrane thickness for vanadium redox flow batteries. Journal of Membrane Science, 437, 108–113. https://doi.org/10.1016/j.memsci.2013.02.007.

Díaz-González, F., Sumper, A., Gomis-Bellmunt, O., & Villafáfila-Robles, R. (2012). A review of energy storage technologies for wind power applications. Renewable and Sustainable Energy Reviews, 16(4), 2154–2171. http://doi.org/ 10.1016/j.rser. 2012.01. 029.

Duncan, R. C. (1988). World Energy Production , Population Growth , and the Road to the Olduvai Gorge, Population and Environment, 22(5), 503–522.

Denholm, P., Ela, E., Kirby, B., & Milligan, M. (2010). The Role of Energy Storage with Renewable Electricity Generation. Contract, NREL/(January), 1–53. https://doi.org/69

Dees, D. W., Battaglia, V. S., & Bélanger, A. (2002). Electrochemical modeling of lithium polymer batteries. Journal of Power Sources, 110(2), 310–320. http://doi.org/10.1016/S0378-7753(02)00193-3.

Doughty, D. H., Butler, P. C., Akhil, A. a, Clark, N. H., & Boyes, J. D. (2010). Batteries for Large-Scale Stationary Electrical Energy Storage. Electrochemical Society Interface, 49–53.

Fisher, G. R., Ieee, M., Anstey, M. R., Viswanathan, V. V, & Perry, M. L. (2014). Redox Flow Batteries : An Engineering Perspective, IEEE, 102(6), 1–24.

Fujimoto, C., Zawodzinski, T., Tang, Z., Pezeshiki, A., Anderson, T., & Pratt, H. (2014). Advanced Membranes for Vanadium Redox Flow Batteries (VRB). Conference of Electricity Energy Storage Program Peer Review.

Fedkiw, P. S., & Watts, R. W. (1984). A mathematical model for the iron/chromium redox battery. Journal of the Electrochemical Society, 131(4), 701–709. https://doi.org/10.1149/1.2115676

Grewal, M., & Andrews, A. (2001). Kalman Filtering: Theory and Practice Using MATLAB. Theory and Practice (Vol. 5). http://doi.org/10.1007/1-4020-0613-6_9753.

Hall, H., & Fasih, A. (2006). Modeling and Fault Diagnosis of Automotive Lead-Acid Batteries. Thesis.

Houser, J., Pezeshki, A., Clement, J. T., Aaron, D., & Mench, M. M. (2017). Architecture for improved mass transport and system performance in redox fl ow batteries. Journal of Power Sources, 351, 96–105. https://doi.org/10.1016/j.jpowsour.2017.03.083.

Haralambopoulos, D. A., & Polatidis, H. (2003). Renewable energy projects: structuring a multi-criteria group decision-making framework. Renewable Energy, 28(6), 961–973. https: //doi.org /10.1016/S0960-1481(02)00072-1.

Hebner, R., Beno, J., & Walls, A. (2002). Flywheel batteries come around again. IEEE spectrum, 39(4), 46-51.

Hopkins, B. J., Smith, K. C., Slocum, A. H., & Chiang, Y. M. (2015). Component-cost and performance based comparison of flow and static batteries. Journal of Power Sources, 293, 1032–1038. https://doi.org/10.1016/j.jpowsour.2015.06.023.

He, H., Xiong, R., Zhang, X., Sun, F., & Fan, J. (2011). State-of-charge estimation of the lithium-ion battery using an adaptive extended Kalman filter based on an improved Thevenin model.

Vehicular Technology, IEEE Transactions on, 60(4), 1461–1469. http://doi.org/10.1109/TVT.2011.2132812.

Huang, K.-L., Li, X., Liu, S., Tan, N., & Chen, L. (2008). Research progress of vanadium redox flow battery for energy storage in China. Renewable Energy, 33(2), 186–192. https://doi.org/10.1016/j.renene.2007.05.025.

Iec. (2009). Executive summary. Electrical Energy Storage White Paper, 39, 11–12. http://doi.org/10.1016/j.icrp.2009.12.007.

Ipsakis, D., Voutetakis, S., Seferlis, P., Stergiopoulos, F., & Elmasides, C. (2009). Power management strategies for a stand-alone power system using renewable energy sources and hydrogen storage. International Journal of Hydrogen Energy, 34(16), 7081–7095. https://doi.org /10.1016 /j.ijhydene.2008.06.051.

Jackey, R., Saginaw, M., Sanghvi, P., Gazzarri, J., Huria, T., & Ceraolo, M. (2013). Battery Model Parameter Estimation Using a Layered Technique : An Example Using a Lithium Iron Phosphate Cell. MathWorks, 1–14. http://doi.org/10.4271/2013-01-1547.

Jyothi Latha, T., & Jayanti, S. (2014a). Ex-situ experimental studies on serpentine flow field design for redox flow battery systems. Journal of Power Sources, 248, 140–146. https://doi.org/10.1016/j.jpowsour.2013.09.084.

Jeon, J. D., Yang, H. S., Shim, J., Kim, H. S., & Yang, J. H. (2014). Dual function of quaternary ammonium in Zn/Br redox flow battery: Capturing the bromine and lowering the charge transfer resistance. Electrochimica Acta, 127, 397–402. https://doi.org/10.1016/j.electacta.2014.02.073

Kear, G., Shah, A. A., & Walsh, F. C. (2012). Development of the all-vanadium redox flow battery for energy storage: A review of technological, Financial and policy aspects. International Journal of Energy Research, 36(11), 1105–1120. https://doi.org/10.1002/er.1863.

Khor, A. C., Mohamed, M. R., Sulaimen, M. H., Daniyal, H., Razali, A. R., Oumer, A. N., &

Leung, P. K. (2016). Numerical investigation on serpentine flow field and rhombus electrolyte compartment of vanadium redox flow battery (V-RFB). ARPN Journal of Engineering and Applied Sciences, 11(10).

Kleeman, L. (1996). Understanding and applying Kalman filtering. Proceedings of the Second Workshop on Perceptive Retrieved from http://www.cs.cmu.edu/~motionplanning /papers/sbp_papers/integrated3/kleeman_kalman_basics.pdf.

Koshizuka, N., Ishikawa, F., Nasu, H., Murakami, M., & Matsunaga, K. (2003). Progress of superconducting bearing technologies for flywheel energy storage systems, 386, 444–450. http://doi.org/10.1016/S0921-4534(02)02206-2.

Kim, D., & Jeon, J. (2015). Study on Durability and Stability of an Aqueous Electrolyte Solution for Zinc Bromide Hybrid Flow Batteries. Journal of Physics: Conference Series, 574(1), 12074. https://doi.org/10.1088/1742-6596/574/1/012074

Liu, H., Xu, Q., Yan, C., & Qiao, Y. (2011). Corrosion behavior of a positive graphite electrode in vanadium redox flow battery. Electrochimica Acta, 56(24), 8783–8790. https://doi.org/10.1016/j.electacta.2011.07.083

Leung, P. K., Mohamed, M. R., Shah, A. A., Xu, Q., & Conde-duran, M. B. (2015). A mixed acid based vanadium e cerium redox fl ow battery with a zero-gap serpentine architecture, Journal of Power Sources, 274, 651–658. https://doi.org/10.1016/j.jpowsour.2014.10.034.

Law, F., & Law, S. (2009). The First, Second, and Third Law of Thermodynamics (ThLaws05.tex), 1–19.

Leung, P., Palma, J., Garcia-quismondo, E., Sanz, L., Mohamed, M. R., & Anderson, M. (2016). Evaluation of electrode materials for all-copper hybrid fl ow batteries. Journal of Power Sources, 310, 1–11. https://doi.org/10.1016/j.jpowsour.2015.12.069.

Luo, X., Wang, J., Dooner, M., & Clarke, J. (2015). Overview of current development in electrical energy storage technologies and the application potential in power system operation. Applied Energy, 137, 511–536. http://doi.org/10.1016/j.apenergy.2014.09.081.

Mahlia, T. M. I., Saktisahdan, T. J., Jannifar, A., Hasan, M. H., & Matseelar, H. S. C. (2014). A review of available methods and development on energy storage; Technology update. Renewable and Sustainable Energy Reviews, 33, 532–545. https://doi.org/10.1016/j.rser.2014.01.068

Mohamed, M. R., Leung, P. K., Sulaiman, M. H. (2015). Performance characterization of a vanadium redox flow battery at different operating parameters under a standardized test-bed system. Applied Energy, 137, 402–412. https://doi.org/10.1016/j.apenergy.2014.10.042.

Mohamed, M. R., Ahmad, H. and Abu Seman, M.N. (2012). State of the art of all-Vanadium Redox Flow Battery : A Research on research prospects. International Review of Electrical Engineering (IREE) 7(5): 5610-5622.

Mohamed, M. R., Ahmad, H., Seman, M. N. A., Razali, S., & Najib, M. S. (2013). Electrical circuit model of a vanadium redox flow battery using extended Kalman filter. Journal of Power Sources, 239, 284–293. https://doi.org/10.1016/j.jpowsour.2013.03.127

Mahlia, T. M. I., Saktisahdan, T. J., Jannifar, A., Hasan, M. H., & Matseelar, H. S. C. (2014). A review of available methods and development on energy storage; Technology update. Renewable and Sustainable Energy Reviews, 33, 532–545. http://doi.org/10.1016/j.rser.2014.01.068.

Miyake, S., & Tokuda, N. (2001). Vanadium redox-flow battery for a variety of applications. 2001 Power Engineering Society Summer Meeting. Conference Proceedings (Cat. No.01CH37262), 1(C), 450–451. https://doi.org/10.1109/PESS.2001.970067.

Oberhofer, A. (2012). Energy Storage Technologies & Their Role in Renewable Integration, (July), 1–42.

Ponce de León, C., Frías-Ferrer, a., González-García, J., Szánto, D. a., & Walsh, F. C. (2006). Redox flow cells for energy conversion. Journal of Power Sources, 160(1), 716–732. https: //doi.org/10.1016/j.jpowsour.2006.02.095.

Parasuraman, A., Lim, T. M., Menictas, C., & Skyllas-Kazacos, M. (2013). Review of material research and development for vanadium redox flow battery applications. Electrochimica Acta, 101, 27–40. https://doi.org/10.1016/j.electacta.2012.09.067

Perry, M. L., & Weber, A. Z. (2016). Advanced Redox-Flow Batteries: A Perspective. Journal of The Electrochemical Society, 163(1), A5064–A5067. https://doi.org/10.1149/2.0101601jes

Rychcik, M., & Skyllas-Kazacos, M. (1988). Characteristics of a new all-vanadium redox flow battery. Journal of Power Sources, 22(1), 59–67. https://doi.org/10.1016/0378-7753(88)80005-3.

Rahman, F., & Skyllas-Kazacos, M. (2009). Vanadium redox battery: Positive half-cell electrolyte studies. Journal of Power Sources, 189(2), 1212–1219. https://doi.org/10.1016/j.jpowsour.2008.12.113.

Rusllim Mohammad, M., Sharkh, S. M., & Walsh, F. C. (2010). Redox flow batteries for hybrid electric vehicles: progress and challenges. 2009 IEEE Vehicle Power and Propulsion Conference, (August 2016), 551–557. https://doi.org/10.1109/VPPC.2009.5289801.

Shah, A. A., & Walsh, F. C. (2009). Electrochimica Acta Non-isothermal modelling of the all-vanadium redox flow battery, 55, 78–89. http://doi.org/10.1016/j.electacta.2009.08.009.

Salerno, D., & Korsunsky, R. (1998). Practical Considerations in the Design of Lithium-Ion Battery Protection Systems. Current, 0(c), 700–707.

Shigematsu, T. (2011). Redox flow battery for energy storage. SEI Technical Review, (73), 4–13. https://doi.org/10.1149/1.3492325.

Shibata, T., Kumamoto, T., Nagaoka, Y., & Kawase, K. (2009). Redox Flow Batteries for the Stable Supply of Renewable Energy, SEI Technical Review, 14–22.

Skyllas-Kazacos, M., Chakrabarti, M. H., Hajimolana, S. a., Mjalli, F. S., & Saleem, M. (2011). Progress in Flow Battery Research and Development. Journal of The Electrochemical Society, 158(8), R55. https://doi.org/10.1149/1.3599565.

Salerno, D., & Korsunsky, R. (1998). Practical Considerations in the Design of Lithium-Ion

Battery Protection Systems. Current, 0(c), 700–707.

Singamsetti, N., & Tosunoglu, S. (2012). A Review of Rechargeable Battery Technologies, Pires, V. F., Romero-cadaval, E., Vinnikov, D., Roasto, I., & Martins, J. F. (2014). Power converter interfaces for electrochemical energy storage systems – A review, 86, 453–475. http://doi.org/10.1016/j.enconman.2014.05.003.

Seyed Schwan Hosseiny. (2011). Vanadium / Air Redox Flow Battery. Faculty of Science and Technology, Membrane Science & Technology. PhD Thesis: 174.

Tüber, K., Oedegaard, A., Hermann, M., & Hebling, C. (2004). Investigation of fractal flow-fields in portable proton exchange membrane and direct methanol fuel cells, Journal of Power Sources, 131, 175–181. https://doi.org/10.1016/j.jpowsour.2003.11.078.

Thaller, L.H. 1976. Electrically rechargeable redox flow cells. Patent, U.S. 3996064.

Tokuda, N., Kumamoto, T., Shigematsu, T., Deguchi, H., Ito, T., Yoshikawa, N., & Hara, T. (1998). Development of a redox flow battery system. SEI Tech Rev, 88–94. Retrieved from http://www.inference.phy.cam.ac.uk/sustainable/refs/SEItechpaper1.pdf.

Vutetakis, D. G. (2001). Avionics Handbook The, 542. http://doi.org/10.1201/9780849384424.

Wold.S,(1974).Spline Fucntions in Data Analysis. Technometrics. http: //doi.org/ 10.1080 /00401706.1974.10489142.

Weber, A. Z., Mench, M. M., Meyers, J. P., Ross, P. N., Gostick, J. T., & Liu, Q. (2011). Redox flow batteries : a review, Journal of Applied, 41(10), 222-348. https://doi.org/10.1007/s10800-011-0348-2.

Winsberg, J., Hagemann, T., Janoschka, T., Hager, M. D., & Schubert, U. S. (2016). Redox-Flow Batteries: From Metals to Organic Redox-Active Materials. Angewandte Chemie - International Edition, 686–711. https://doi.org/10.1002/anie.201604925.

Xu, Q., Zhao, T. S., & Leung, P. K. (2013). Numerical investigations of flow field designs for vanadium redox flow batteries. Applied Energy, 105, 47–56. https://doi.org/10.1016/j.apenergy.2012.12.041.

Yu, D., & Yuvarajan, S. (2005). Electronic circuit model for proton exchange membrane fuel cells ☆, 142, 238–242. http://doi.org/10.1016/j.jpowsour.2004.09.041.

Yin, C., Gao, Y., Guo, S., & Tang, H. (2014). A coupled three dimensional model of vanadium redox flow battery for flow field designs. Energy, 74(C), 886–895. https://doi.org/10.1016/j.energy.2014.07.066.

You, X., Ye, Q., & Cheng, P. (2016). Scale-up of high power density redox flow batteries by introducing interdigitated flow fields. International Communications in Heat and Mass Transfer, 75, 7–12. https://doi.org/10.1016/j.icheatmasstransfer.2016.03.021.

Yang, H. S., Park, J. H., Ra, H. W., Jin, C. S., & Yang, J. H. (2016). Critical rate of electrolyte circulation for preventing zinc dendrite formation in a zinc-bromine redox flow battery. Journal of Power Sources, 325, 446–452. https://doi.org/10.1016/j.jpowsour.2016.06.038.

YIlmaz, I., & Yuksek, a. G. (2008). An example of artificial neural network (ANN) application for indirect estimation of rock parameters. Rock Mechanics and Rock Engineering, 41(5), 781–795. http://doi.org/10.1007/s00603-007-0138-7.

Zhang, C., Liu, J., Sharkh, S. M., & Zhang, C. (2009). Identification of dynamic model parameters for lithium-ion batteries used in hybrid electric vehicles. International Symposium on Electric Vehicles, 1, 1–11. http://doi.org/10.3772/j.issn.1006-6748.2010.01.002.

Zhang, C., Jiang, J., Zhang, W., & Sharkh, S. M. (2012). Estimation of state of charge of lithium-ion batteries used in HEV using robust extended Kalman filtering. Energies, 5(4), 1098–1115. http://doi.org/10.3390/en5041098.

Zhao, P., Zhang, H., Zhou, H., Chen, J., Gao, S., & Yi, B. (2006). Characteristics and performance of 10 kW class all-vanadium redox-flow battery stack, Journal of Power Sources, 162, 1416–1420. https://doi.org/10.1016/j.jpowsour.2006.08.016.

Zeng, Y. K., Zhao, T. S., An, L., Zhou, X. L., & Wei, L. (2015). A comparative study of all-vanadium and iron-chromium redox flow batteries for large-scale energy storage. Journal of Power Sources, 300, 438–443. https://doi.org/10.1016/j.jpowsour.2015.09.100.